Cell Reports
Article

Asymmetric Localization of *Cdx2* mRNA during the First Cell-Fate Decision in Early Mouse Development

Maria Skamagki,[1,3,5] Krzysztof B. Wicher,[1,3] Agnieszka Jedrusik,[1] Sujoy Ganguly,[2,4] and Magdalena Zernicka-Goetz[1,*]
[1]The Gurdon Institute, University of Cambridge, Tennis Court Road, Cambridge, CB2 1QN, United Kingdom
[2]Department of Applied Mathematics and Theoretical Physics, University of Cambridge, Wilberforce Road, Cambridge CB3 0WA, United Kingdom
[3]These authors contributed equally to this work
[4]Present address: Max Planck Institute for Molecular Cell Biology and Genetics; Pfotenhauerstrasse 108; 01307 Dresden, Germany
[5]Present address: Memorial Sloan Kettering Cancer Center, 1275 York Avenue, New York 10065, NY, USA
*Correspondence: mz205@cam.ac.uk
http://dx.doi.org/10.1016/j.celrep.2013.01.006

SUMMARY

A longstanding question in mammalian development is whether the divisions that segregate pluripotent progenitor cells for the future embryo from cells that differentiate into extraembryonic structures are asymmetric in cell-fate instructions. The transcription factor *Cdx2* plays a key role in the first cell-fate decision. Here, using live-embryo imaging, we show that localization of *Cdx2* transcripts becomes asymmetric during development, preceding cell lineage segregation. *Cdx2* transcripts preferentially localize apically at the late eight-cell stage and become inherited asymmetrically during divisions that set apart pluripotent and differentiating cells. Asymmetric localization depends on a *cis* element within the coding region of *Cdx2* and requires cell polarization as well as intact microtubule and actin cytoskeletons. Failure to enrich *Cdx2* transcripts apically results in a significant decrease in the number of pluripotent cells. We discuss how the asymmetric localization and segregation of *Cdx2* transcripts could contribute to multiple mechanisms that establish different cell fates in the mouse embryo.

INTRODUCTION

Asymmetric localization of specific transcripts is a common posttranscriptional mechanism for regulating gene activity in various model systems (Holt and Bullock, 2009; St Johnston, 2005, Meignin and Davis, 2010). Such asymmetric localization and then segregation of messenger RNA (mRNA) in cell division are often important for cell-fate determination (Li et al., 1997; Melton, 1987; Neuman-Silberberg and Schüpbach, 1993). However, whether any asymmetric localization and segregation of transcripts occur in early mammalian embryos is currently unknown.

Segregation of the first two cell lineages in the mouse embryo is initiated at the eight- to 16-cell-stage transition when blastomeres undertake divisions to generate inside cells that will form pluripotent inner cell mass (ICM) and outside cells that will form trophectoderm (TE) (Johnson and Ziomek, 1981; Bruce and Zernicka-Goetz, 2010). The ICM gives rise to cells of the future body, and the TE gives rise to an extraembryonic tissue with an essential role in patterning the embryo and building the placenta. Divisions that generate ICM and TE progenitor cells were cautiously termed "differentiative" (Johnson and Ziomek, 1981) because it was unknown whether such divisions are asymmetric in transmitting cell-fate instructions or whether inside and outside cells follow different fates only because of the differential positions assumed by the cells. In contrast, divisions that generate only TE progenitor cells were termed "conservative."

A number of transcription factors that are important for distinguishing the ICM and TE lineages become differentially expressed between inside and outside cells, which are precursors of these first two cell lineages. Of these, *Cdx2* and *Eomes* have increased expression in outside cells (Russ et al., 2000; Strumpf et al., 2005), and *Oct4*, *Sox2*, and *Nanog* have progressively increased expression in inside cells (Avilion et al., 2003; Chambers et al., 2003; Mitsui et al., 2003; Palmieri et al., 1994). *Cdx2* is critical for initiating this cell-fate diversification. Preventing *Cdx2* expression leads to an increased expression of pluripotency genes in outside cells and improper development of the TE (Strumpf et al., 2005; Jedrusik et al., 2008). One established means of regulating the differential expression of *Cdx2* between inside and outside cells is to exert transcriptional control in response to differential cell position when the ICM and TE precursors segregate from each other. This is achieved through nuclear localization of Yes-associated protein (YAP) in outside cells to permit *Tead4*-mediated transcription of *Cdx2* (Yagi et al., 2007; Nishioka et al., 2008). The retention of YAP in the cytoplasm of inside cells, in part through the activity of the Hippo pathway, restrains transcription of *Cdx2* in inside cells (Nishioka et al., 2009). As a result of differential expression of *Cdx2*, factors required for pluripotency are downregulated in outside but not inside cells (Niwa et al., 2005). The effect of cell position upon the regulation of *Cdx2* expression is therefore well established.

The mechanisms behind the first differential expression of *Cdx2* among blastomeres at the eight-cell stage are less well understood (Jedrusik et al., 2008; Ralston and Rossant, 2008). However, this differential expression is important because it significantly biases cell fate: cells with higher levels of CDX2 contribute preferentially to the TE, and those with lower levels contribute preferentially to the ICM (Jedrusik et al., 2008). The orientation of cell divisions that govern whether cells are allocated to the TE or ICM is influenced by cell polarization (Plusa et al., 2005). However, the effect of cell polarity on CDX2 remains largely unknown.

Here, we provide evidence for temporal and spatial localization and segregation of *Cdx2* transcripts that precede the segregation of the ICM and TE lineages. Using a sensitive assay to follow transcripts in living mouse embryos, we found that *Cdx2* mRNA becomes preferentially localized apically at the late eight-cell stage and inherited asymmetrically at the eight- to 16-cell transition. We define the localization sequence within the *Cdx2* mRNA and show that *Cdx2* mRNA localization depends on apical polarization and the microtubule and actin cytoskeletons. Preventing *Cdx2* mRNA localization leads to the upregulation of CDX2 protein in inside cells, which consequently decreases the number of pluripotent cells. Our results indicate that "differentiative" divisions in the mouse embryo contribute to the asymmetry of cell-fate instruction: they prevent inside cells from inheriting *Cdx2* transcripts, thereby permitting the development of pluripotency while adding support to the differentiation program of outside cells.

RESULTS

Spatial and Temporal Localization of *Cdx2* Transcripts

CDX2 is a key transcription factor that constitutes an essential switch in the first cell-fate decision. It becomes expressed differentially upon the differentiative divisions at the eight- to 16-cell transition. *Cdx2* expression in outside cells is critical for TE specification and has to be suppressed in inside cells to allow development of pluripotency. In order to determine the mechanism that regulates this differential *Cdx2* expression, we first examined in detail the spatial and temporal distribution of *Cdx2* transcripts by fluorescent in situ hybridization (FISH). We found that before embryo compaction occurs, *Cdx2* mRNA distributes evenly within the cells (n = 56), but in contrast, upon compaction at the late eight-cell stage, *Cdx2* mRNA becomes localized asymmetrically along the apical-basal axis (n = 144; Figure 1A). Apical localization of *Cdx2* mRNA was evident in 81% (117/144) of cells in compacted embryos (a significantly greater proportion than in uncompacted embryos in which none of the cells showed apical localization of *Cdx2* mRNA; n = 0/56, χ^2 test, $p < 0.001$). The remaining 19% of cells (27/144) showed either no localization (8%) or a distribution that was ambiguous (11%; Figure S1A). In order to quantitate the spatial distribution of *Cdx2* transcripts, we used a computational approach to measure the polarization of the FISH signal (Park et al., 2012). In this method, apical distribution is characterized by small values of the angle between the polarization index (PI) vector and the apical-basal axis (θ), and by relatively high positive values of the basal-apical polarization (BA) vector (see Extended Experimental Procedures). The analyses yielded mean values for θ of $126^\circ \pm 7^\circ$ /SEM/ and $23^\circ \pm 3^\circ$, and the BA values of -0.32 ± 0.05 /SEM/ and 0.51 ± 0.04 for uncompacted (n = 49) and compacted (n = 65) embryos, respectively (t test, $p < 0.001$; Figures 1B–1D), indicating that *Cdx2* transcripts localize toward the apical region upon compaction. Apical localization was not observed for transcripts of two other transcription factors examined at this stage, *Dab2* (n = 33, $\theta = 121^\circ \pm 8^\circ$ and BA = -0.14 ± 0.02) and *Gata3* (n = 25, $\theta = 89^\circ \pm 11^\circ$ and BA = 0.01 ± 0.03), which distributed evenly (Figures 1A and 1C). Thus, *Cdx2* transcripts acquire a polarized distribution preceding ICM and TE lineage segregation.

Dynamics of *Cdx2* Transcript Localization

The finding that *Cdx2* mRNA localizes apically in the late eight-cell embryo raised several questions: (1) What are the dynamics of spatial localization of *Cdx2* transcripts? (2) Do *Cdx2* transcripts partition asymmetrically during differentiative cell-fate-directing divisions? (3) What is the mechanism behind the *Cdx2* transcripts localization? (4) What might be the role of asymmetrically localized *Cdx2* transcripts? To address these questions, we first had to establish an assay to follow localization of *Cdx2* mRNA in living mouse embryos. To that end, we synthesized fluorescently labeled *Cdx2* and control mRNAs, and injected them into individual eight-cell embryo blastomeres (Figures 1E and 1F) that had compacted and were therefore expected to undergo apical-basal polarization (Johnson and Ziomek, 1981). We found that labeled control mRNAs transcribed from the pBluescript plasmid backbone (n = 15; Figure 1F), from green fluorescent protein (GFP, n = 12; Figure 3H), or from Nanog complementary DNA (cDNA; not shown) showed no regional localization in any focal plane. In contrast, labeled full-length *Cdx2* mRNA with intact 5′ and 3′ untranslated regions (UTRs) showed significant accumulation in the apical region of cells (54%, n = 52; χ^2 test, $p < 0.001$; Figure 1E; Movie S1). In the remaining cells, transcripts were observed either in a perinuclear location (25%) or dispersed throughout the cytoplasm (21%). Quantitation of the fluorescence intensity along the apical-basal axis of each cell at the focal plane of its maximum intensity revealed an apical concentration of the signal in *Cdx2* but not in control mRNA injected embryos (Figures S1B and S1C). This apical concentration of *Cdx2* mRNA was also observed on other focal planes. Finally, we coinjected *Cdx2* and pBluescript RNAs labeled with two different fluorescent dyes, and this confirmed their differential localization (n = 7; Figure S1D).

To determine whether the above three broad locations of *Cdx2* mRNA represented final or intermediate positions of transcripts, we needed to follow their spatial dynamics in live embryos. To that end, we injected labeled full-length *Cdx2* mRNA into 34 individual cells in a second cohort of compacted eight-cell embryos, and carried out confocal time-lapse microscopy beginning 1.5 hr after injection. At the beginning of the time-lapse series, 16 out of 34 injected cells already showed apical localization of *Cdx2* transcripts. Of the remaining embryos, 11 had transcripts first enriched in the perinuclear space (Figure 1G, time points 0 and 20 min; Movie S1) that within the next 20–30 min translocated toward the apical region and spread along the apical cell surface (Figure 1G, time points 40

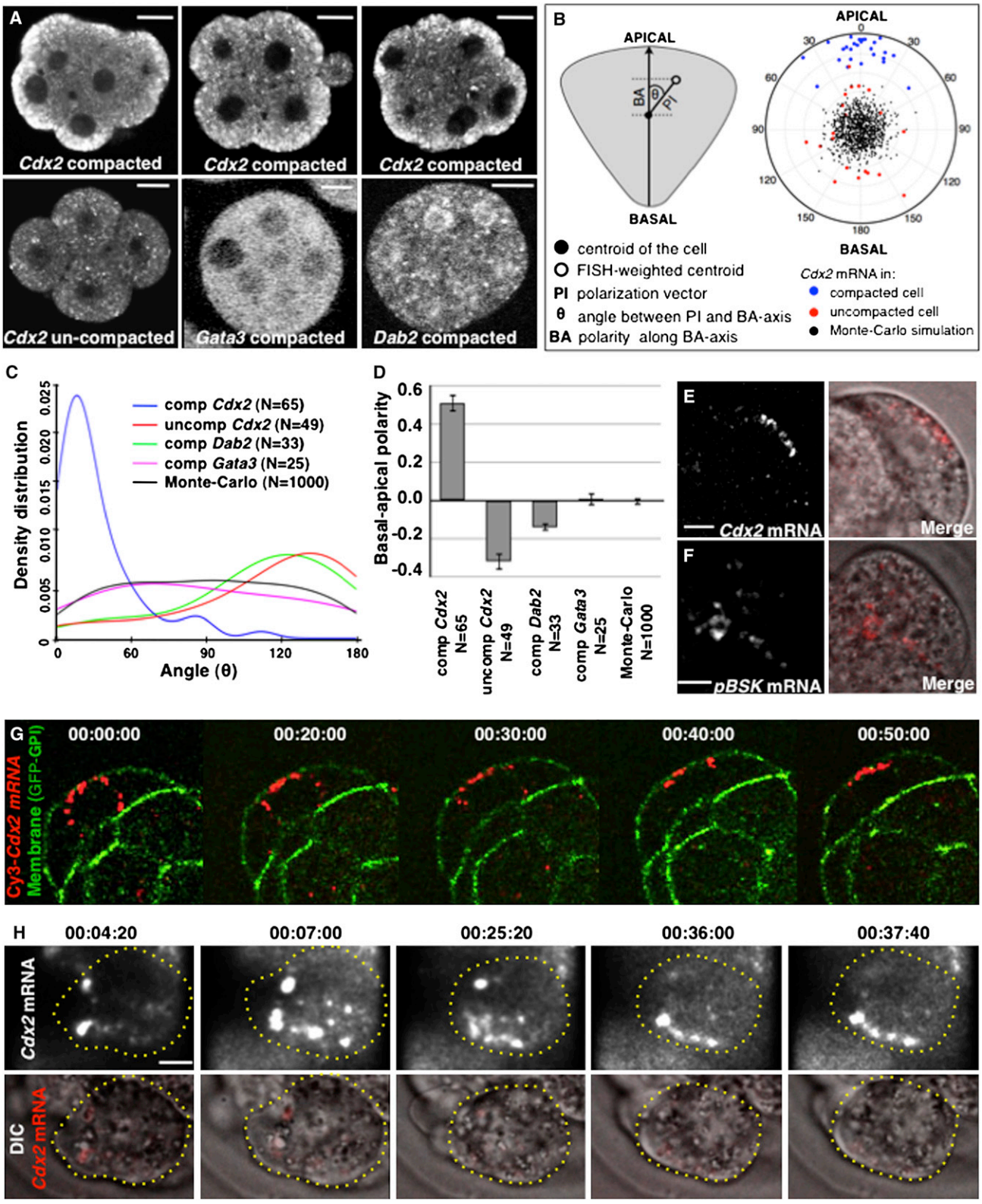

Figure 1. Exogenous *Cdx2* Transcripts Recapitulate Endogenous *Cdx2* Transcript Localization

(A) Representative images of endogenous *Cdx2* (n = 56 uncompacted and n = 144 compacted), Dab2 (n = 17 compacted), and Gata3 (n = 14 compacted) mRNAs detected by FISH in eight-cell embryos. Scale bar, 10 μm.

(legend continued on next page)

and 50 min). In only seven out of the 34 cells (20%) we could not detect any specific localization of *Cdx2* mRNA. Similar behavior of *Cdx2* mRNA was observed in newly formed outside cells at the 16-cell stage (Figure 1H; Movie S2). In agreement with the FISH results, *Cdx2* mRNA injected into eight-cell blastomeres assessed prior to embryo compaction did not show any particular localization (n = 17; Figure S1E). Thus, the proportion of cells in which exogenous *Cdx2* mRNA showed transient perinuclear or stable apical localization (80%, n = 86) is significant (χ^2 test, $p < 0.001$ in comparison with pBluescript plasmid backbone) and similar to the proportion that displayed apical localization of endogenous *Cdx2* mRNA detected by FISH at the late eight-cell stage (81%, n = 144, χ^2 test, $p < 0.001$ in comparison with uncompacted embryos). Thus, exogenous *Cdx2* mRNA, like endogenous mRNA, acquires a polarized distribution along the apical-basal axis preceding cell divisions leading to ICM and TE lineage segregation.

Partitioning of *Cdx2* Transcripts at the Eight- to 16-Cell-Stage Transition

It is known that localizations of mRNAs can lead to an asymmetric inheritance by daughter cells upon cell division in many model systems. To determine whether this might be so in the mouse embryo, we followed the segregation of *Cdx2* transcripts during divisions that generate cells of distinct fates. To that end, we injected fluorescent *Cdx2* mRNA and imaged its distribution by time-lapse microscopy. We found that in differentiative divisions, in which cleavage furrows are perpendicular to the apical-basal axis and one daughter inherits the majority or entirety of the outer-facing apical domain, *Cdx2* transcripts were inherited by the cell with the predominant apical domain (n = 10/10; Figure 2A; Figure S2A; Movie S3). In contrast, during conservative divisions, which generate outer daughter cells with apical domains equivalent in size, *Cdx2* transcripts were inherited by both daughters in similar amounts (n = 11/11; Figure 2B; Figure S2B; Movie S4). This apical localization of transcripts could appear temporarily disrupted during mitosis but was then reestablished within 30–40 min of cytokinesis. We also attempted to catch embryos at the eight- to 16-cell transition to examine the distribution of endogenous *Cdx2* by FISH. We found that at prometaphase, *Cdx2* transcripts were enriched in apical regions, and at anaphase/telophase they were enriched in the cytoplasm destined for the outside rather than the inside daughter cell (17/34; Figures 2C and 2D; Figures S2C and S2D). The enrichment of *Cdx2* transcripts in outside versus inside cells could also be detected by quantitative PCR (qPCR) following the cell division (Figure S2E). These results suggest that more *Cdx2* transcripts become distributed to cells that initiate differentiation into TE rather than to cells that develop as pluripotent ICM.

Cdx2 Transcript Localization Depends on a *cis* Element within the Coding Region

It is known that specific sequence elements within targeted mRNAs are able to direct them to subcellular localizations. These *cis*-acting elements (also known as localization elements or zipcodes) frequently reside in the 3′ untranslated region (UTR) of a targeted mRNA but can also be found within the 5′UTR or open reading frame (ORF) (Jambhekar and Derisi, 2007). To identify the element required for localization of *Cdx2* mRNA, we first generated a series of truncated forms of the *Cdx2* gene and followed their localization (Figure 3A). We found that whereas truncated RNA missing the 5′UTR and part of the ORF (499ORF-3′UTR) could localize to the apical region (n = 9/18, χ^2 test, $p = 0.994$ compared with the wild-type (WT) mRNA; Figures 3B and 3J), truncated RNA missing the 3′UTR and part of the ORF (5′UTR-439ORF) could not, and was always distributed throughout the cytoplasm (n = 13/13; χ^2 test, $p < 0.001$ compared with the WT mRNA; Figures 3C and 3J). Because RNA containing only the ORF construct also localized apically (n = 8/14, χ^2 test, $p = 1$ compared with the WT mRNA; Figures 3D and 3J), we argued that a localization element must reside within the ORF of *Cdx2*, and, more specifically, within the last 499 nt. To define the localization element more tightly, we generated two further constructs comprising the 3′UTR and shorter segments (326 or 97 nt) of the 3′ part of the ORF (362ORF-3′UTR and 97ORF-3′UTR). Both of these RNAs distributed apically (n = 12/18, χ^2 test, $p = 0.502$ [Figures 3J and S3A], and n = 19/31, χ^2 test, $p = 0.665$ [Figures 3E and 3J], respectively, compared with the WT mRNA), suggesting that the 97 nt element at the 3′ of the ORF is sufficient to drive the localization.

To confirm the functionality of this element, we fused it to either RNA transcribed from the pBluescript plasmid or from GFP cDNA and determined whether it could direct localization of these unrelated RNAs. We found that the 97 nt element was able to confer apical localization upon these RNAs (n = 38/69, χ^2 test, $p = 1$ [Figures 3F–3H], and n = 16/24, χ^2 test, $p = 0.422$

(B) Quantification of the distribution of *Cdx2* transcripts. Polar coordinates for individual cells are expressed as a single point defined by vector PI and angle θ on a polar graph. The PI vector is defined by the center of gravity of the cell and the center of gravity of the FISH signal. This vector shows an angular displacement, θ (the angular coordinate), from the apical-basal (polar) axis. The radial coordinate (PI) can be alternatively expressed along the apical-basal (polar) axis as the value BA. Apical localization of *Cdx2* mRNA in compacted blastomeres (n = 27) is represented by the clustering of blue dots around 0°; red dots represent *Cdx2* mRNA in individual cells before compaction (n = 20), and black dots represent a Monte Carlo simulation of random localization.
(C) Density distributions of values for angles θ for indicated transcripts (measured as described in B for individual cells).
(D) Representation of the distribution as the average value (±SEM) of the polar coordinate (BA) for the indicated transcripts. This has a positive value when directed apically and is negative when basal.
(E and F) Localization of exogenous labeled RNAs for full-length *Cdx2* mRNA (E; n = 52) and control mRNA (F; n = 12) injected into eight-cell embryo cells and imaged 1.5–2 hr after injection. Scale bar, 10 μm.
(G) Stills from a representative movie of a compacted eight-cell blastomere injected with labeled *Cdx2* mRNA. Time points are presented in hr:min:s format. Scale bar, 20 μm.
(H) Dynamics of *Cdx2* mRNA localization after cell division of the eight-cell blastomere. A cell outline is presented with a dashed line. Scale bar, 5 μm.
See also Figure S1, and Movies S1 and S2.

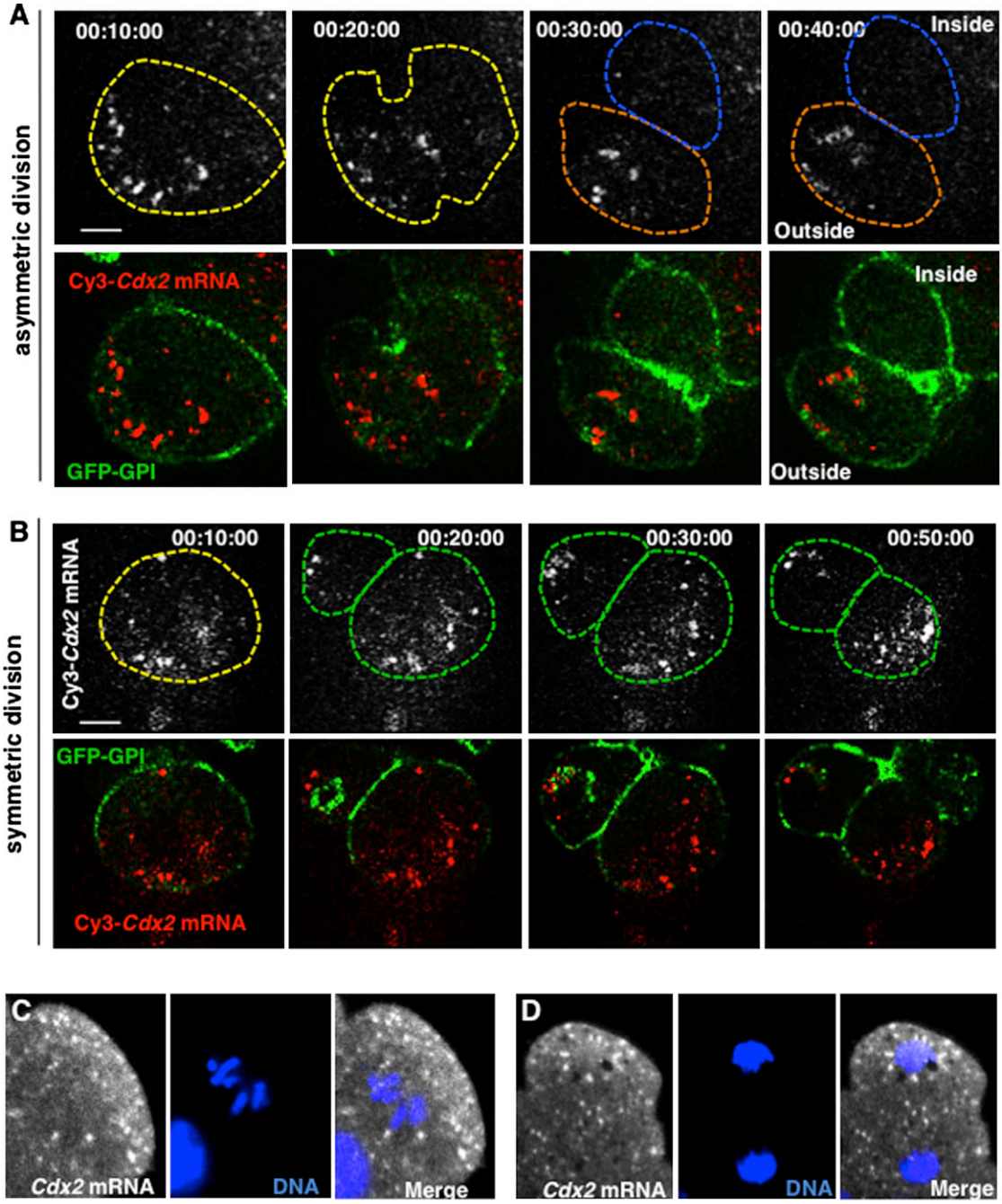

Figure 2. *Cdx2* mRNA Localization at the Eight- to 16-Cell Transition

(A and B) Live imaging of exogenous Cy3-labeled *Cdx2* mRNA distribution during asymmetric (A) and symmetric (B) divisions. Time points are presented in hr:min:s format.

(C and D) FISH detection of endogenous *Cdx2* mRNA during the eight- to 16-cell transition in mitotic cells (C) and during telophase (D). Scale bar, 10 μm.

See also Figure S2, and Movies S3 and S4.

[Figure 3I], respectively, compared with the full-length transcript). Together, these results suggest that a region of the *Cdx2* transcript comprising the last 97 nt of the ORF is sufficient for localization. Moreover, because the 97 nt element in these last two constructs was placed out of the reading frame, translation of polypeptide from this element does not seem to play a role in apical localization.

Some RNA localization elements form hairpin stem loops (Hamilton and Davis, 2007), which led us to consider whether this might be the case for the 97 nt *Cdx2* localization signal.

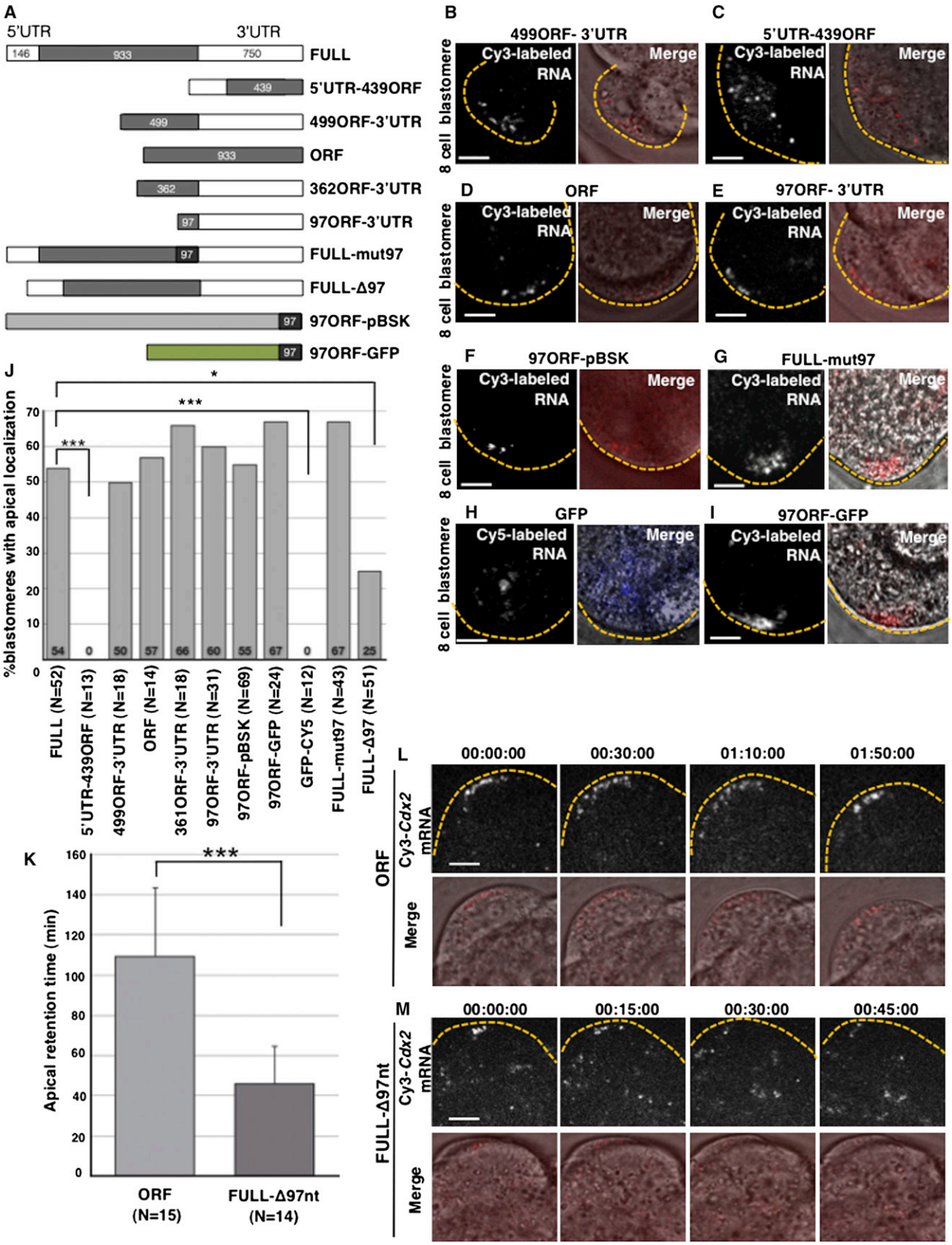

(legend on next page)

We found that the lowest free-energy structure predicted by the *mfold* program (Extended Experimental Procedures) contains two stem loops, one of which (comprising the last 51 nt) has a high probability of base-pairing (Figure S3B) and contains runs of purines in the predicted stem that are similar to those previously reported to be important for localization signal activity (Bullock et al., 2010). To test whether this predicted structure plays a role, we introduced ten mutations that should abolish a hairpin loop but preserve the amino acid sequence (Figure S3C). This mutated RNA (FULL-mut97) was still able to localize apically (n = 29/43, χ^2 test, p = 0.178 compared with WT mRNA; Figures 3G and 3J), suggesting that this putative structure is not required.

Finally, to verify that the 97 nt sequence is necessary for *Cdx2* mRNA localization, we created a full-length *Cdx2* construct deleted only for the 97 nt element (*Δ97nt*). We found that the localization of labeled *Δ97nt* RNA was significantly reduced to 25% of injected cells (n = 13/51, χ^2 test, $p < 0.05$; Figure 3J) in comparison with WT mRNA, but not totally abolished. This prompted us to examine the dynamics of localization of the *Δ97nt* form by time-lapse microscopy. This revealed that the *Δ97nt* form was transported apically (n = 14; Figures 3L and 3M; Movies S5 and S6). However, its average time of persistence at the apical region was significantly decreased to 46 min relative to 109 min for the WT ORF construct (n = 15, t test, $p < 0.001$; Figure 3K). Together, these results indicate that the 97 nt element is sufficient to drive the apical localization of *Cdx2* transcripts and is also required for anchorage and/or stability of the transcripts at the apical cortex. Interestingly, the 97 nt at the 3′ terminal part of *Cdx2* coding sequence is highly conserved in placental mammals (Figure S3D).

Cdx2 Transcript Localization Requires an Intact Cytoskeleton

The actin and microtubule networks participate in the transport and anchoring of transcripts at target sites in many model systems (López de Heredia and Jansen, 2004). We therefore wished to determine whether this is also the case for *Cdx2* mRNA. To disrupt the microtubule network, we used nocodazole and first confirmed that a 30 min treatment of eight-cell embryos was sufficient for this purpose (n = 20/20; Figures 4A and 4C) as previously reported (Johnson and Maro, 1984). We found that this treatment prevented the apical localization of *Cdx2* transcripts in all compacted eight-cell embryos (n = 0/18 embryos, $\theta = 166° \pm 3°$ and BA = -1.42 ± 0.08), whereas vehicle-treated controls were unaffected (n = 6/7 embryos, $\theta = 33° \pm 12°$ and BA = 1.01 ± 0.20, χ^2 test, $p < 0.001$). This was not due to decreased stability of the *Cdx2* transcript, because the nocodazole did not significantly change the *Cdx2* mRNA level determined by qRT-PCR (pairwise fixed reallocation randomization test, p (H1) = 0.12; Figure S4).

We next established that a 60-min treatment with cytochalasin-D resulted in partial depolymerization of the filamentous actin, as was evident from the disorganization of cortical actin, some embryo decompaction, and a decrease in overall cytoplasmic staining (n = 15/15; Figure 4B). This partial depolymerization of actin was sufficient to disrupt the apical localization of *Cdx2* transcripts in all embryos examined (n = 0/12 embryos, $\theta = 140° \pm 13°$ and BA = -0.82 ± 0.2), whereas control embryos were not affected (n = 12/12 embryos, $\theta = 33° \pm 12°$ and BA = 1.01 ± 0.20; χ^2 test, $p < 0.001$). The disruption of the actin cytoskeleton also caused some perturbation in microtubule organization, and vice versa, and both of these treatments caused mislocalization of atypical protein kinase C (aPKC) from apical poles (n = 15/15 and n = 17/18 embryos, respectively, for both χ^2 tests, $p < 0.001$ compared with untreated embryos; Figures S4B and S4C).

Prompted by the fact that depolymerization of microtubules had a strong effect on *Cdx2* transcript localization, we wished to determine whether a microtubule-dependent molecular motor could be involved. To that end, we injected compacted eight-cell blastomeres with either anti-pan-kinesin or anti-dynein intermediate chain antibodies, and 30–60 min later with labeled *Cdx2* mRNA. None of the blastomeres injected with the pan-kinesin antibodies showed apical localization of transcripts 1.5–2 hr after injections (n = 0/20, χ^2 test, $p < 0.001$ in comparison with *Cdx2* mRNA injection in control embryos; Figure 4D), whereas antibodies against dynein had no observable effect (n = 4/7, Fisher's exact test, $p < 0.05$ in comparison with *Cdx2* mRNA injection in control embryos; Figure 4E). We confirmed the successful injection of antibodies by immunostaining (data not shown). Together, these results suggest that *Cdx2* transcript localization requires either one or both of the microtubule and actin networks, which are interdependent at this developmental stage, and the activity of a motor protein of the kinesin superfamily.

Cdx2 Transcript Localization Requires Cell Polarization

The apical enrichment of the *Cdx2* transcripts upon apical-basal polarization suggested a possible role of cell polarization in this process. To determine whether this is the case, we first overexpressed the dominant-negative form of aPKC zeta (dn-aPKC), which disrupts cell polarization at the eight-cell stage (Plusa et al., 2005), together with GFP mRNA as a lineage marker. We coinjected these constructs into one cell at the late two-cell stage to restrict the effect to half of the embryo. The embryos were allowed to develop to the late eight-cell stage,

Figure 3. A *Cdx2* mRNA Localization Element Resides in the Last 97 nt of the Coding Sequence

(A) Schematic representation of the *Cdx2* and fusion constructs along with their controls used for injections.

(B–I) Representative images of localization patterns observed for the truncated forms of *Cdx2* mRNA. Scale bar, 10 μm.

(J) Quantification of the injection experiments and numbers of injected blastomeres. Statistically significant differences compared with the control are marked with asterisks (χ^2 test, *$p < 0.05$, ***$p < 0.001$).

(K) Quantification of average (±SEM) apical persistence time of ORF and Δ97 *Cdx2* transcripts (t test, $p < 0.001$).

(L and M) Stills from representative movies of labeled *Cdx2* ORF RNA (L; n = 15) and Δ97 form (M; n = 14) injected into compacted blastomeres of an eight-cell embryo. Time points (hr:min:s) starting 40 min postinjection are indicated above the panels. Scale bar, 10 μm.

See also Figure S3, and Movies S5 and S6.

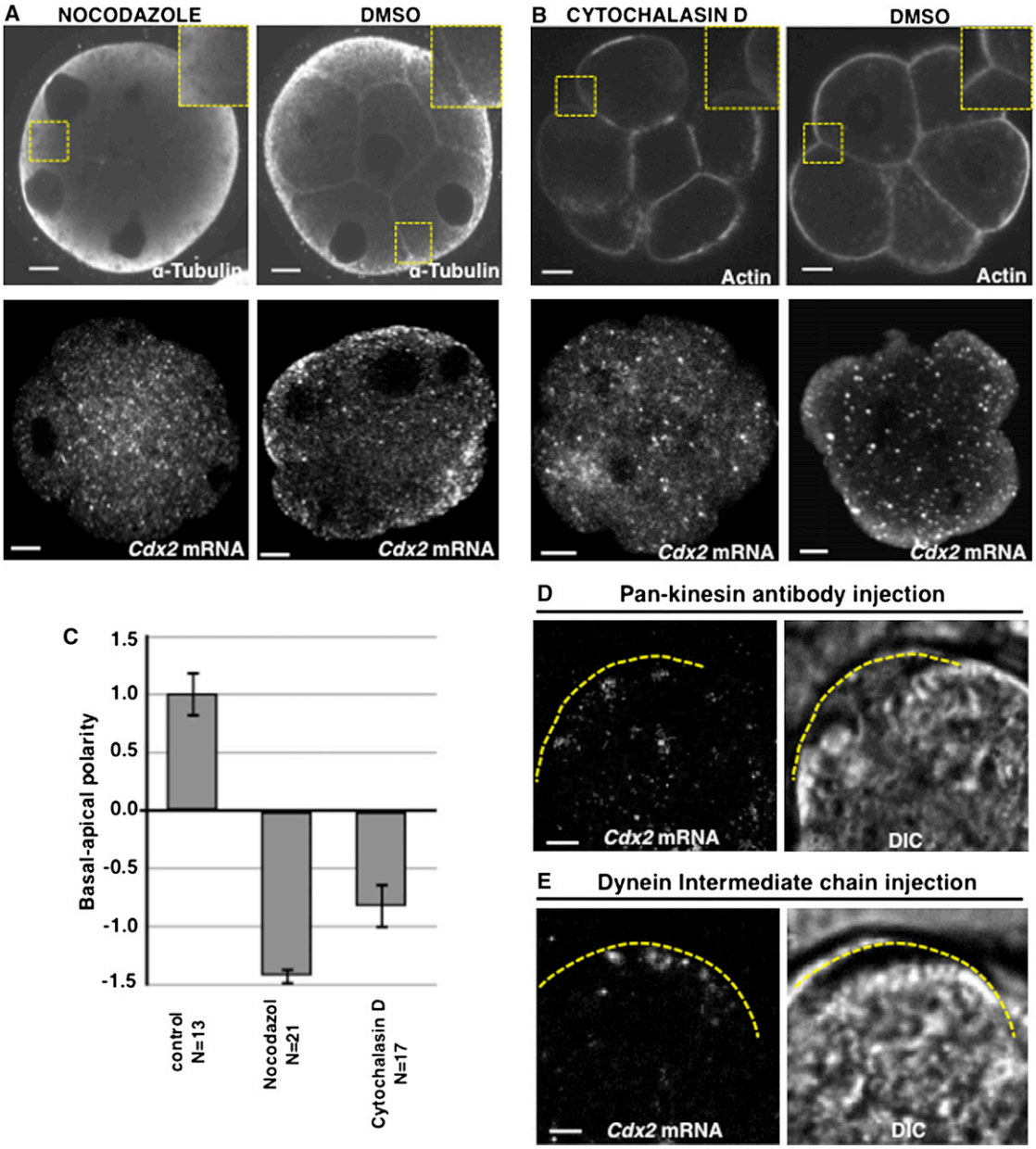

Figure 4. Localization of *Cdx2* mRNA Requires an Intact Cytoskeleton

(A and B) Embryos treated with nocodazole (A) and cytochalasin D (B) and with the vehicle control (DMSO). FISH detection of endogenous *Cdx2* mRNA in eight- to 16-cell-stage embryos (lower panels in A [18 embryos] and B [12 embryos]). Immunostaining for α-tubulin (upper panels in A; n = 14). F-actin staining with phalloidin (upper panels in B; n = 15). Scale bar, 15 μm.

(C) Quantification of the polarization, represented as average BA value (±SEM), in individual cells of embryos treated with nocodazole and cytochalasin D.

(D and E) Localization of labeled *Cdx2* mRNA following injection of anti-pan-kinesin (D; n = 0/20) or dynein intermediate chain (E; n = 4/7) antibodies. Scale bar, 5 μm.

See also Figure S4.

and then *Cdx2* mRNA was detected by FISH in one group and aPKC protein was detected by immunofluorescence in a second group (Figures 5A and 5B). Following downregulation of aPKC in half of the embryo, there were 2-fold fewer cells with apical *Cdx2* transcripts than in control embryos (n = 18/56 cells, seven embryos, versus n = 51/80 cells, ten embryos; χ^2 test, $p < 0.001$). Consistently, aPKC distribution was perturbed in cells descended from the injected blastomere in the second cohort of embryos (Figure 5C). Filamentous actin staining in the cytoplasm appeared stronger following treatment with dn-aPKC (Figure 5C), although there was no effect on the microtubule network (Figure S5).

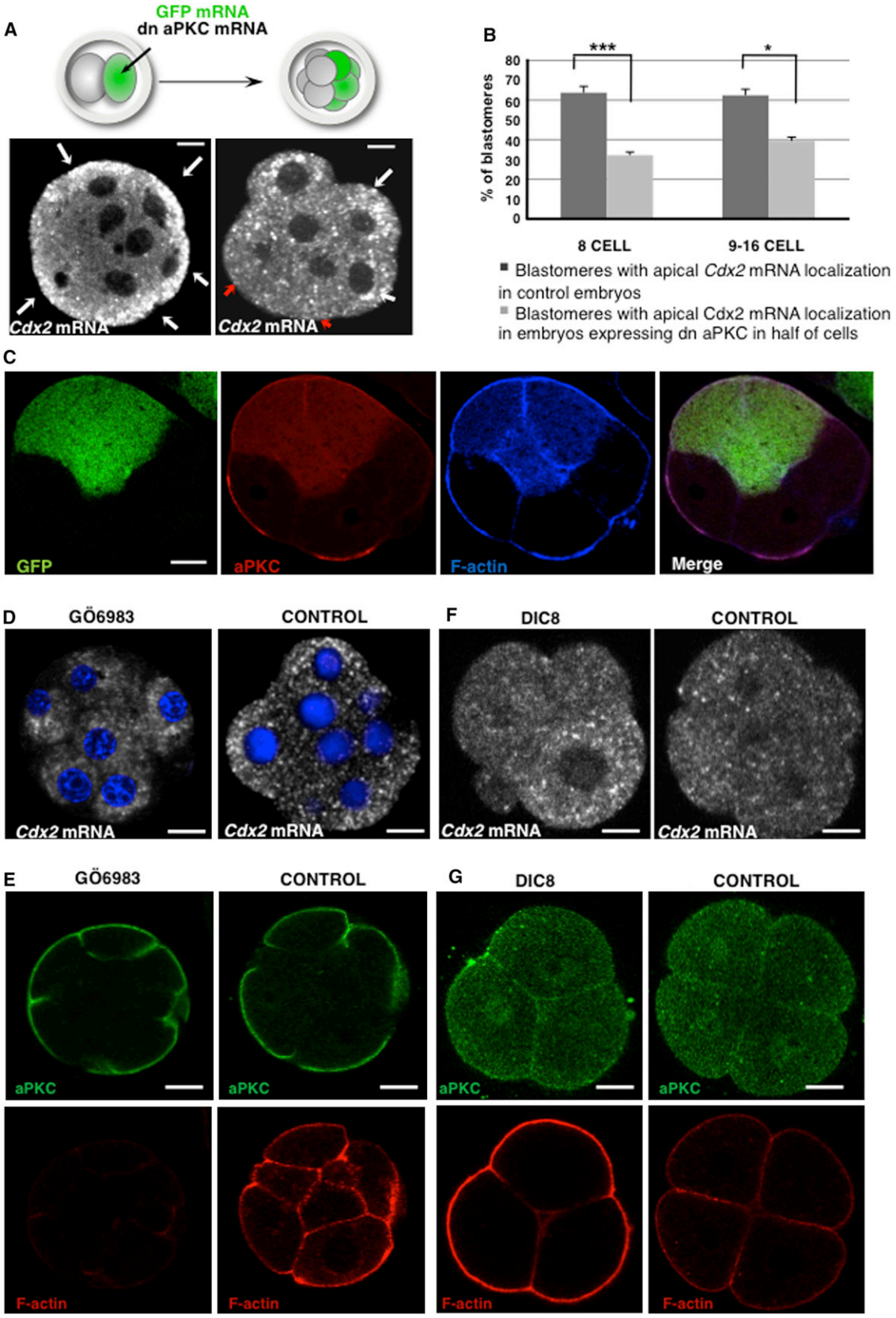

(legend on next page)

In a second series of experiments, we confirmed the requirement for aPKC activity on *Cdx2* mRNA localization by treating eight-cell embryos with Gö6983, an inhibitor of aPKC activity (particularly PKC zeta). A 60-min treatment with Gö6983 completely abolished *Cdx2* mRNA localization (n = 0/8 embryos, $\theta = 136^\circ \pm 12^\circ$ and BA = -0.46 ± 0.13, χ^2 test, $p < 0.01$; Figure 5D) compared with vehicle only-treated control embryos (n = 6/6 embryos, $\theta = 18^\circ \pm 4^\circ$ and BA = 1.33 ± 0.11, Fisher's exact test, $p < 0.001$). The inhibitor did not affect the localization of aPKC but had a strong effect on actin, as evidenced by loss of phalloidin staining of cytoplasmic and cortical/microvilli (Figure 5E).

Finally, we wondered whether induction of premature embryo compaction would be sufficient for *Cdx2* mRNA localization. We therefore induced compaction by treating four-cell embryos with DiC8, a diacylglycerol analog and an activator of PKCs, and monitored compaction by phalloidin staining and differential interference contrast (DIC) microscopy (data not shown). Such prematurely induced compaction did not lead to either premature apical localization of aPKC in all examined embryos (n = 0/6 embryos; Fisher's exact test $p < 0.05$; Figure 5G) or localization of *Cdx2* transcripts (n = 0/6 embryos, Fisher's exact test $p < 0.05$; Figure 5F). These results indicate that *Cdx2* mRNA localization requires aPKC kinase activity that is associated with cell polarization at the eight-cell stage.

Preventing *Cdx2* Transcript Localization Leads to Expression of CDX2 Protein in ICM

Having observed that *Cdx2* mRNA is inherited mainly by outside cells upon cell division at the eight- to 16-cell transition, we wished to determine whether this is important for cell-fate specification. To address this, we needed to prevent *Cdx2* mRNA localization and determine the effect on cell fate. To achieve this, we injected blastomeres with the *97nt* RNA containing the *Cdx2* localization element to compete for localization with endogenous *Cdx2* transcripts. To determine the efficiency of this approach, we first coinjected a 10× molar excess of the *97nt* RNA with labeled *Cdx2* mRNA, and found a 5-fold reduction of cells showing apical *Cdx2* mRNA in comparison with control cells injected with unrelated RNA of comparable size (χ^2 test, $p < 0.001$; Figures 6A and 6B). Having established this proof of principle, we injected all blastomeres at the four-cell stage with *97nt* (comp) RNA or with unrelated RNA (control), and cultured embryos until the blastocyst stage. We found that the embryos injected with control RNA expressed CDX2 only in the TE (n = 14 embryos), as expected. In contrast, in >75% of embryos injected with the *97nt* RNA, CDX2 protein was clearly detectable in one or more inside cells (n = 10/13 embryos, χ^2 test, $p < 0.001$; Figure 6C). Thus, interfering with the *Cdx2* transcripts' localization machinery results in CDX2-positive inside cells.

Preventing CDX2 Transcript Localization Decreases the Number of Pluripotent Cells

In order to determine the developmental effects of *Cdx2* transcript mislocalization, we performed an experiment similar to the one described above, but this time allowed embryos to develop further so that we could assess the precise cell lineage allocation (Figures 6D and 6E). We found that injection of the *97nt* RNA reduced the number of epiblast (NANOG-expressing) cells significantly (t test, $p < 0.001$) compared with control embryos (average values of 5.2 versus 9.2 cells, respectively; n = 20). In contrast, development of the TE and primitive endoderm was not significantly affected (Figure 6F).

To address how mislocalization of CDX2 to inside cells can lead to fewer epiblast cells, we overexpressed CDX2 in inside cells (or outside cells as control) together with a lineage marker, Rhodamine Dextran (DxRed), to follow their fate directly by four-dimensional (4D) time-lapse microscopy (Figure S6). This revealed that inside cells injected with *Cdx2* mRNA at the 16- to 32-cell stage developed normally at first and gave rise to 37 inside progeny (n = 17 embryos). However, as the embryos reached the mature blastocyst stage, 95% of CDX2-expressing cells underwent cell death (n = 35/37; Figures 6G, 6K, and 6L). The timing of the apoptosis of CDX2-positive cells coincided with the onset of apoptosis known to occur in normal development (Handyside and Hunter, 1986; Morris et al., 2010). The two CDX2-positive cells that survived gave rise to primitive endoderm (Figure 6J). In contrast, outside cells injected with *Cdx2* mRNA gave rise to 34 cells, of which only three (9%) underwent apoptosis (n = 3/34; Figures 6H and 6K). To eliminate the possibility that injection of inside cells per se might lead to cell death, we injected inside cells with DxRed alone (n = 19 embryos). These cells gave rise to 40 inside progeny, 37% of which died (n = 15/40; Figures 6I and 6K). This suggests that the increased death of inside cells could be due in part to their greater sensitivity to injection per se, but most likely it reflects the known incidence of cell death within the ICM. This is because the rate of cell death in inside CDX2-positive cells was significantly greater than in both control groups of cells (Fisher's exact test, two-tailed, $p < 0.001$; Figure 6K), indicating that

Figure 5. Disruption of Cell Polarity Abolishes Apical Localization of *Cdx2* mRNA

(A–C) *dn-aPkc* mRNA along with lineage tracer (GFP mRNA) was injected into one blastomere of two-cell embryos that were then cultured until the late eight-cell stage.

(A) FISH detection of endogenous *Cdx2* mRNA in control (left panel; n = 51/80, ten embryos) and dn-aPKC injected (right panel; n = 18/56, seven embryos) embryos. *Cdx2* mRNA localized apically is indicated by white arrows, and its absence in some blastomeres is shown by red arrows. Scale bar, 5 μm.

(B) Quantification of the blastomeres that showed apical *Cdx2* mRNA localization in the experiment shown in (A) and (B) (mean value ± SEM; Student's t test; $^*p < 0.05$, $^{***}p < 0.001$).

(C) Effect of dn-aPKC (marked with GFP fluorescence, first panel) on localization of aPKC (second panel) and actin (third panel). Scale bar, 15 μm.

(D and E) Effect of aPKC inhibition with Gö6983 in compacted eight-cell blastomeres on *Cdx2* mRNA localization (D; n = 8 embryos) and on actin (E, upper panel; n = 6 embryos) and aPKC (E, lower panel; n = 6 embryos) localization. Scale bar, 15 μm.

(F and G) Effect of premature compaction of four-cell embryos resulting from activation of PKCs with DiC8 on mRNA localization (F; n = 6 embryos), and on actin (G, upper panel; n = 6 embryos) and aPKC (G, lower panel; n = 6 embryos) localization. Scale bar, 15 μm.

See also Figure S5.

Cell PRESS
Open ACCESS

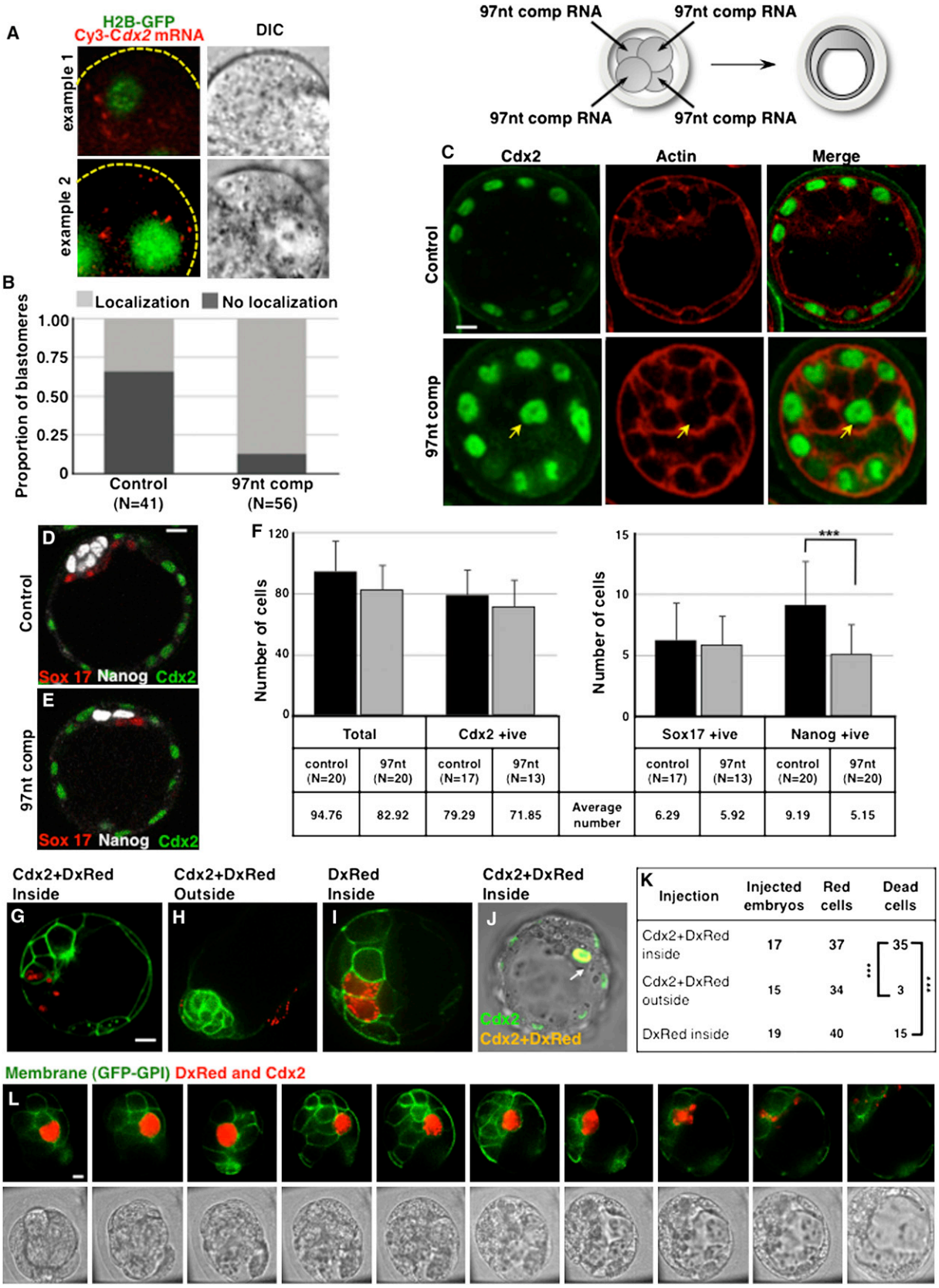

(legend on next page)

a high CDX2 level is not well tolerated in the ICM. Together, our results suggest that preventing *Cdx2* mRNA apical localization leads to a decrease in pluripotent cell numbers.

DISCUSSION

The results we present here indicate that transcripts for *Cdx2*, a critical factor in the first cell-fate decision in the mouse embryo, preferentially localize asymmetrically toward the apical region of blastomeres at the late eight-cell stage. *Cdx2* mRNA localization depends on a 97 nt *cis* element within the ORF and requires intact actin and microtubule cytoskeletons as well as apical-basal cell polarization. We find that the asymmetric localization of *Cdx2* mRNA leads to the acquisition of more *Cdx2* by outside cells compared with inside cells. This asymmetry likely contributes to the elevated CDX2 expression that directs the development of outside cells into TE. But perhaps more importantly, it can serve to ensure that inside cells do not inherit *Cdx2* transcripts and consequently CDX2 protein, thus enabling them to develop as the pluripotent cell lineage. Our findings therefore indicate that differentiative divisions are truly asymmetric because they lead to the asymmetric segregation of at least one factor that is critical for cell differentiation: *Cdx2* mRNA. When cells divide conservatively, each daughter inherits similar levels of *Cdx2* mRNA, and thus, from this perspective, these divisions can be considered symmetric. After the completion of cell division, *Cdx2* transcripts relocalize to the apical regions of cells. This may be important for ensuring that in the second round of differential divisions, inside cells do not become enriched with CDX2.

Our studies of *Cdx2* transcript localization dynamics indicate that the mechanism of their localization depends on a 97 nt element within the coding region of *Cdx2*. This is suggested by three observations: First, a 97 nt element from the 3′ end of the ORF is sufficient to position *Cdx2* mRNA apically. Second, other RNAs tagged with this 97 nt element localize apically. Third, *Cdx2* transcripts lacking this element show only transient localization, indicating that the 97 nt element provides anchorage/stability of the transcript in the apical region. Although localization elements are more usually placed within the UTRs, they are known to reside within the ORFs of targeted mRNAs in other model systems (Jambhekar and Derisi, 2007). This 97 nt is highly conserved in the *Cdx2* genes of placental mammals, raising the possibility that *Cdx2* mRNA might also localize in other species. Although it remains unknown which parts of the 97 nt element are essential for the apical anchorage, our mutational studies suggest that is not a predicted loop structure. Our results also suggest that another apical transporting sequence may lie outside of the 97 nt element, but that this sequence is unable to mediate the efficient anchorage or stability of the transcript at this site. Such binary elements mediating redundant and/or developmentally orchestrated functions in other localizing mRNAs have been reported (Simmonds et al., 2001).

Our results indicate that the maintenance or stability of the *Cdx2* mRNA at the apical region requires the integrity of the microtubule and actin cytoskeletons. Transcript localization also requires cell polarization because disruption of aPKC zeta, which is critical for cell polarity at this stage (Plusa et al., 2005), leads to the loss of *Cdx2* mRNA's apical enrichment. Additionally, we find that overexpression of a component of the subcortical maternal complex FLOPED (Li et al., 2008), which interferes with eight-cell embryo polarization, results in *Cdx2* transcript relocalization to basolateral regions (Figure S5B). Whether this effect of cell polarity on mRNA localization is direct or indirect remains unknown. Importantly, we find that experimentally induced premature embryo compaction cannot induce the localization of *Cdx2* transcripts, which suggests that correct cell polarization at the eight-cell stage, rather than compaction per se, is required.

We can detect asymmetric *Cdx2* transcripts in ~80% of cells in late eight-cell-stage embryos. This raises the question of what happens in the remaining 20% of cells. At least four possibilities can be considered. First, it is possible that polarization of *Cdx2* mRNA does not arise simultaneously in all blastomeres. This would accord with the known lack of synchrony of preimplantation development. A second possibility is that *Cdx2* transcript distribution does not polarize in all cells, which would lead to some inside cells inheriting *Cdx2* mRNA. This would explain the fraction of inside cells reported to contain *Cdx2* protein (Dietrich and Hiiragi, 2007). Third, *Cdx2* mRNA localization might be prevented by disruption of the apical region through the process of cell injection (Morris, 2011; Yamanaka, 2011). We consider this possibility to be less likely, because we examined *Cdx2* mRNA asymmetry 1.5–2 hr after injection, when polarity is likely

Figure 6. Mislocalization of *Cdx2* mRNA in the Eight-Cell Embryo Results in CDX2 Protein in Inside Cells and a Decrease in Epiblast Cell Number

(A) Coinjection of excess of RNA containing competitor *Cdx2* 97 nt localization signal (*97nt comp*) with labeled *Cdx2* mRNA abolishes apical localization of *Cdx2* mRNA, which now localizes to basolateral regions.

(B) Quantification of cells showing apical localization of labeled *Cdx2* mRNA upon coinjection of *97nt comp* (competitor; n = 56) or control unrelated RNA of similar size (n = 41); the difference is statistically significant (χ^2 test, $p < 0.001$).

(C–F) All cells of the four-cell embryo were injected with control or *97nt comp* RNA and allowed to develop until the early (C) or mature blastocyst (D–F) stage.

(C) Representative images of embryos stained for *Cdx2* (green) and actin (red). Yellow arrow marks an inside cell positive for *Cdx2* in the embryo injected with *97nt comp* RNA (n = 10/13); control injected embryos do not express *Cdx2* in inside cells (n = 0/14).

(D and E) Examples of embryos injected with control (D) and *97nt comp* (E) RNA stained for CDX2 (green), SOX17 (red), or NANOG (white).

(F) Quantification of the percentage (±SEM) of cells positive for *Cdx2*, Sox17, or Nanog in blastocyst (~96-cell stage).

(G–L) Single inside (G, J, and L; n = 17) or outside (H; n = 15) cells of a 16-32 cell embryos injected with *Cdx2* mRNA and DxRed (G, H, and J) or with DxRed alone (I; n = 19). Progeny of inside cells injected with *Cdx2* mRNA shows nuclear CDX2 at blastocyst stage (H, arrow; green plus red = yellow). Scale bar, 10 μm.

(K) Summary of injection data (Fisher's exact test, ***$p < 0.001$).

(L) Time-lapse series of an embryo with one inside cell injected with *Cdx2* mRNA and DxRed.

See also Figure S6.

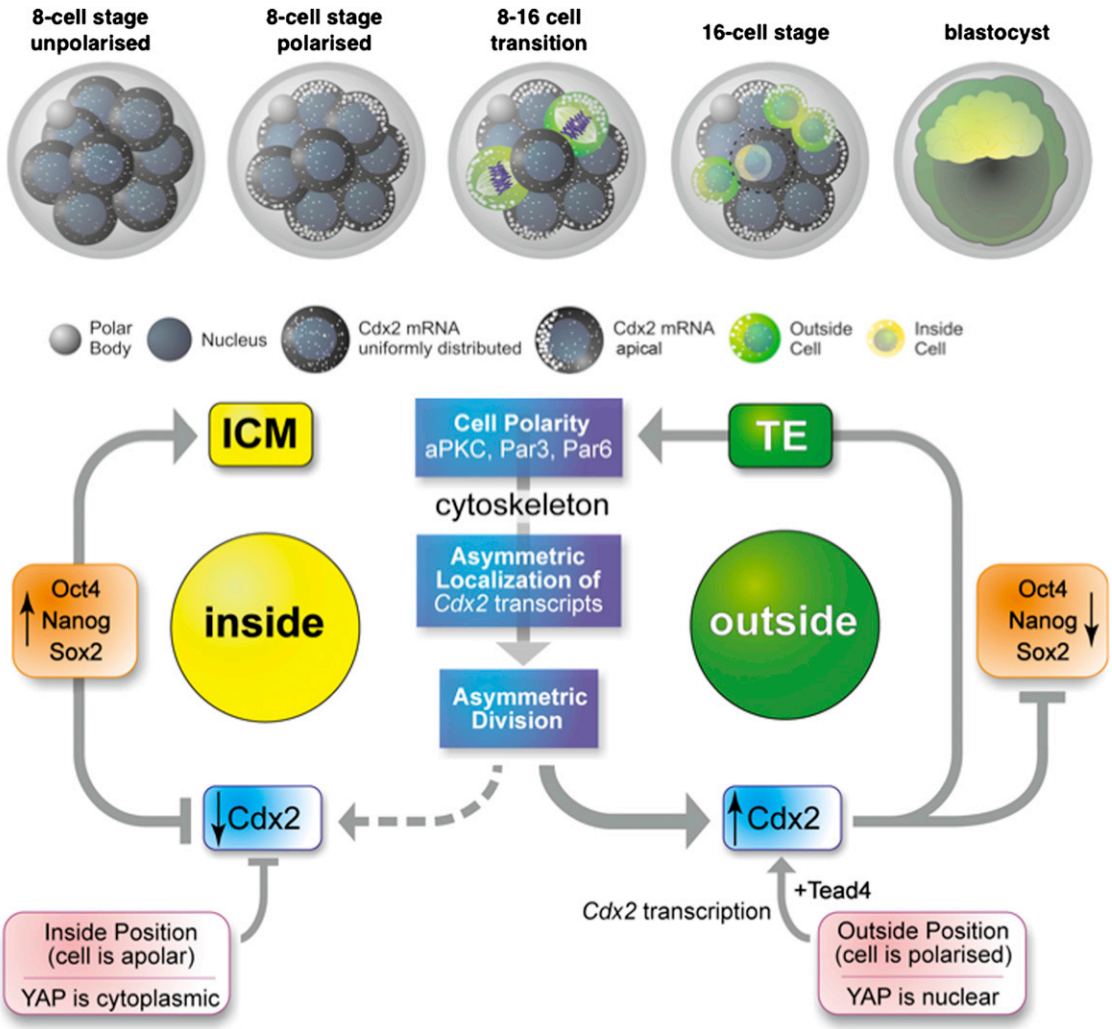

Figure 7. Working Model for How the Localization and Partitioning of *Cdx2* Transcripts together with Differential Transcription Lead to Lineage Segregation

(Top) Symmetric cell division generates two outside cells (green) that inherit similar amounts of *Cdx2* transcripts. Asymmetric division generates an outside daughter that inherits more *Cdx2* transcripts (green) than the inside daughter (yellow).

(Bottom) Cell polarization leads to the asymmetric localization of *Cdx2* transcripts and their differential inheritance, contributing to elevated levels of CDX2 in outside cells (as we show here). This CDX2 asymmetry is then reinforced by a transcriptional response to TEAD4 and the nuclear localization of YAP in outside cells (Yagi et al., 2007; Nishioka et al., 2008, 2009). In turn, the elevated CDX2 level reinforces cell polarization (Jedrusik et al., 2008) and represses the expression of pluripotency factors (Niwa et al., 2005) to promote differentiation into the TE lineage. In contrast, the reduced CDX2 level in inside cells is a consequence of (1) reduced inheritance of *Cdx2* transcripts, (2) prevention of *Cdx2* transcription as a result of the cytoplasmic retention of YAP, and (3) the repressive effects of OCT4 and NANOG that promote pluripotent fate.

to have been restored. Fourth, polarization of *Cdx2* transcripts might not be detectable in blastomeres in which *Cdx2* expression is very low. Indeed expression of CDX2 is heterogeneous at the eight-cell stage (Jedrusik et al., 2008; Ralston and Rossant, 2008).

It has been suggested that *Cdx2* mRNA is provided not only zygotically but also maternally (Jedrusik et al., 2010; Wu et al., 2010), and that simultaneous depletion of both maternal and zygotic *Cdx2* pools has a stronger effect on TE development than depletion of only the zygotic pool (Jedrusik et al., 2010). The maternal pool of *Cdx2* appears not to be essential on its own (Blij et al., 2012). However, whether the maternal provision of *Cdx2* message is superfluous or helpful in enhancing TE specification is not clear and awaits a thorough comparison of the developmental dynamics of embryos with both maternal and zygotic pools of *Cdx2* eliminated versus embryos in which only the zygotic pool is removed. It is important to note that the work we present here does not distinguish between maternal and zygotic pools of *Cdx2* mRNA.

The asymmetric localization of *Cdx2* mRNA is likely to have important implications for the first cell lineage specification (Figure 7), for two main reasons. First, polarized localization of *Cdx2*

transcripts can contribute to increased levels of CDX2 protein in outside cells, which is critical for TE development (Strumpf et al., 2005; Jedrusik et al., 2008). Such initial asymmetry in *Cdx2* mRNA would be further enhanced through the nuclear translocation of YAP, which together with TEAD4 promotes *Cdx2* expression via transcriptional control (Yagi et al., 2007; Nishioka et al., 2008, 2009). Second, asymmetric localization and inheritance of *Cdx2* mRNA is likely to contribute to the development of pluripotency of inside cells by ensuring low levels of CDX2 in these cells, which downregulates pluripotency gene expression (Niwa et al., 2005). In support of this, our results show that interference with *Cdx2* mRNA localization leads to CDX2 protein synthesis in inside cells, and that this interferes with their development along the pluripotent lineage. We therefore suggest that assignment of TE identity and de facto ICM identity during the first fate decision draws upon more than one mechanism. It is perhaps for this reason that mammalian embryos can call upon regulative developmental mechanisms more effectively than their more deterministic metazoan relatives. In agreement with this, the preferential inheritance of *Cdx2* transcripts by outside, TE-destined cells might provide an elegant cell-fate "insurance policy" that would help negate any inappropriate Hippo signaling input. Such inappropriate signaling could arise from cell divisions that are neither parallel nor perpendicular to the apical-basal axis (Sutherland et al., 1990) and affect the size of cell-to-cell contact domains on which Hippo signaling might depend. In conclusion, our results add support to the notion that cell polarity and CDX2-mediated cell fate are interdependent, and bring together earlier models proposed for cell-fate specification (Figure 7). At the same time, they raise a new possibility that the polarized localization of mRNA for other cell-fate factors at the eight-cell stage might contribute to cell-fate specification in mouse embryo.

EXPERIMENTAL PROCEDURES

Embryo Collection and Culture

Embryos were collected from F1 (C57Bl6 × CBA) females mice superovulated with 10 IU of PMSG (Intervet) and 10 IU of human chorionic gonadotropin (HCG; Intervet) 48 hr later and mated with F1 or with EGFP-H2B (Hadjantonakis and Papaioannou, 2004) males. The embryos were recovered in M2 medium with 4 mg/mL BSA and cultured in KSOM medium under paraffin oil at 37.5°C in 5% CO_2 as previously described (Bischoff et al., 2008). Eight-cell embryos were obtained by collecting four-cell embryos 56–61 hr after HCG injection and culturing either for a further 1–2 hr or for 10–12 hr after division to the eight-cell stage.

Whole-Mount RNA FISH

FISH was performed as previously described (Chazaud et al., 2006). Digoxigenin-labeled RNA probes were generated by direct in vitro transcription using the T_7 MEGA-Script kit (Ambion). Details of the protocol are provided in Extended Experimental Procedures.

Synthesis of Fluorescently Labeled, Capped RNA and Microinjections

In vitro synthesis of mRNA was performed as previously described (Bullock and Ish-Horowicz, 2001). Linearized plasmid template was transcribed in a solution containing 0.4 mM ATP, 0.4 mM CTP, 0.36 mM UTP, 0.04 mM Cy3-UTP (Perkin Elmer), 0.12 mM GTP, and m7G(5′)ppp(5′)G cap analog (Ambion) using T_3 (pBluescriptRN3P) or T_7 (pBluescriptSK+) RNA polymerases (Roche) according to the manufacturer's instructions. The resultant RNA was treated with DNase I (Ambion), purified using the MegaClear kit (Ambion), and precipitated with NH_4OAc/EtOH. One or more blastomeres of compacted eight-cell embryos were injected at a concentration of 500 ng/μL. The integrity of the RNA was checked by electrophoresis before injection. Injection of fluorescently labeled *Drosophila* transcripts (kindly provided by Simon Bullock) adopted a dispersed distribution similar to that observed for our control RNAs. None of the synthetic RNAs we used impaired development.

Constructs and mRNA Injection

A full-length ORF *Cdx2* cDNA clone containing the majority of the 3′ and 5′ UTRs was obtained from Geneservice (Cambridge, UK) and cloned into pBluescript SK + plasmid. Truncated forms of *Cdx2* were obtained by subcloning of respective fragments. *dnaPKC*, *Floped*, and GFP mRNAs were prepared and injected into blastomeres as previously described (Zernicka-Goetz et al., 1997). The embryos were cultured until the eight-cell stage and then processed for FISH and immunostaining. To obtain statistically significant numbers, all experiments were performed on embryos from more than a single batch, and several independent experiments were conducted.

Cdx2 mRNA (50 ng/μl) was injected into cells of 16- to 32-cell embryos expressing membrane-bound GFP protein with DxRed as a lineage tracer. The embryos were imaged as described previously (Morris et al., 2010).

97nt comp RNA (total length of ~200 nt) was transcribed from a DNA construct comprising the mRNA localization signal of *Cdx2* in pBluescript vector. Control RNA consisted of ~200 nt of a 5′ sequence of GFP mRNA. The RNAs were injected into all four-cell embryo cells, which were then allowed to develop until blastocyst stage.

Image Analysis

To calculate the PI of the FISH signal, a previously described algorithm (Park et al., 2012) was adopted and implemented in JRuby as an ImageJ plugin or in MATLAB using MathWorks (Extended Experimental Procedures). Fluorescence intensity plots were derived using MATLAB. All data analyses were performed on raw images.

4D Imaging

Time-lapse imaging of labeled RNA was performed using a spinning-disk confocal microscope (Marianas; Intelligent Imaging Innovations) with Slidebook (Intelligent Imaging Innovations) software and a camera (QuantEM 512SC; Yokogawa). Images were taken with 500 ms exposure in focal planes spaced 3.5 μm apart and using a 63 × Plan-Neofluar water immersion objective.

Immunofluorescence

Embryos were fixed in 4% paraformaldehyde in PBS containing 0.1% Tween20 for 30 min at 37°C or in 10% DMSO in methanol for 5 min at −20°C. The samples were washed in 0.1% Tween20 in PBS (PBST), permeabilized in 0.25% Triton X-100 in PBS for 20 min at room temperature, washed in PBST, and incubated in blocking solution (3% BSA in PBST) for 2 hr at room temperature as previously described (Jedrusik et al., 2008). The antibodies used are listed in Extended Experimental Procedures.

SUPPLEMENTAL INFORMATION

Supplemental Information includes Extended Experimental Procedures, six figures, and six movies and can be found with this article online at http://dx.doi.org/10.1016/j.celrep.2013.01.006.

LICENSING INFORMATION

ACKNOWLEDGMENTS

We are grateful to Simon Bullock, David Glover, Claire Chazaud, Rui Pires Martins, Alexander Bruce, Kitai Kim, Isabel Palacios, and Alejandra Gardiol for help and advice. This work was supported by a Wellcome Trust Senior Research Fellowship to M.Z.G. M.S. was funded by the Greek State Scholarships Foundation.

Received: February 4, 2012
Revised: June 1, 2012
Accepted: January 7, 2013
Published: January 31, 2013

REFERENCES

Avilion, A.A., Nicolis, S.K., Pevny, L.H., Perez, L., Vivian, N., and Lovell-Badge, R. (2003). Multipotent cell lineages in early mouse development depend on SOX2 function. Genes Dev. *17*, 126–140.

Bischoff, M., Parfitt, D.E., and Zernicka-Goetz, M. (2008). Formation of the embryonic-abembryonic axis of the mouse blastocyst: relationships between orientation of early cleavage divisions and pattern of symmetric/asymmetric divisions. Development *135*, 953–962.

Blij, S., Frum, T., Akyol, A., Fearon, E., and Ralston, A. (2012). Maternal Cdx2 is dispensable for mouse development. Development *139*, 3969–3972.

Bruce, A.W., and Zernicka-Goetz, M. (2010). Developmental control of the early mammalian embryo: competition among heterogeneous cells that biases cell fate. Curr. Opin. Genet. Dev. *20*, 485–491.

Bullock, S.L., and Ish-Horowicz, D. (2001). Conserved signals and machinery for RNA transport in Drosophila oogenesis and embryogenesis. Nature *414*, 611–616.

Bullock, S.L., Ringel, I., Ish-Horowicz, D., and Lukavsky, P.J. (2010). A'-form RNA helices are required for cytoplasmic mRNA transport in Drosophila. Nat. Struct. Mol. Biol. *17*, 703–709.

Chambers, I., Colby, D., Robertson, M., Nichols, J., Lee, S., Tweedie, S., and Smith, A. (2003). Functional expression cloning of Nanog, a pluripotency sustaining factor in embryonic stem cells. Cell *113*, 643–655.

Chazaud, C., Yamanaka, Y., Pawson, T., and Rossant, J. (2006). Early lineage segregation between epiblast and primitive endoderm in mouse blastocysts through the Grb2-MAPK pathway. Dev. Cell *10*, 615–624.

Dietrich, J.E., and Hiiragi, T. (2007). Stochastic patterning in the mouse preimplantation embryo. Development *134*, 4219–4231.

Hadjantonakis, A.K., and Papaioannou, V.E. (2004). Dynamic in vivo imaging and cell tracking using a histone fluorescent protein fusion in mice. BMC Biotechnol. *4*, 33.

Hamilton, R.S., and Davis, I. (2007). RNA localization signals: deciphering the message with bioinformatics. Semin. Cell Dev. Biol. *18*, 178–185.

Handyside, A.H., and Hunter, S. (1986). Cell division and death in the mouse blas- tocyst before implantation. Rouxs Arch. Dev. Biol. *195*, 519–526.

Holt, C.E., and Bullock, S.L. (2009). Subcellular mRNA localization in animal cells and why it matters. Science *326*, 1212–1216.

Jambhekar, A., and Derisi, J.L. (2007). Cis-acting determinants of asymmetric, cytoplasmic RNA transport. RNA *13*, 625–642.

Jedrusik, A., Parfitt, D.E., Guo, G., Skamagki, M., Grabarek, J.B., Johnson, M.H., Robson, P., and Zernicka-Goetz, M. (2008). Role of Cdx2 and cell polarity in cell allocation and specification of trophectoderm and inner cell mass in the mouse embryo. Genes Dev. *22*, 2692–2706.

Jedrusik, A., Bruce, A.W., Tan, M.H., Leong, D.E., Skamagki, M., Yao, M., and Zernicka-Goetz, M. (2010). Maternally and zygotically provided Cdx2 have novel and critical roles for early development of the mouse embryo. Dev. Biol. *344*, 66–78.

Johnson, M.H., and Maro, B. (1984). The distribution of cytoplasmic actin in mouse 8-cell blastomeres. J. Embryol. Exp. Morphol. *82*, 97–117.

Johnson, M.H., and Ziomek, C.A. (1981). The foundation of two distinct cell lineages within the mouse morula. Cell *24*, 71–80.

Li, L., Baibakov, B., and Dean, J. (2008). A subcortical maternal complex essential for preimplantation mouse embryogenesis. Dev. Cell *15*, 416–425.

Li, P., Yang, X., Wasser, M., Cai, Y., and Chia, W. (1997). Inscuteable and Staufen mediate asymmetric localization and segregation of prospero RNA during Drosophila neuroblast cell divisions. Cell *90*, 437–447.

López de Heredia, M., and Jansen, R.P. (2004). mRNA localization and the cytoskeleton. Curr. Opin. Cell Biol. *16*, 80–85.

Meignin, C., and Davis, I. (2010). Transmitting the message: intracellular mRNA localization. Curr. Opin. Cell Biol. *22*, 112–119.

Melton, D.A. (1987). Translocation of a localized maternal mRNA to the vegetal pole of Xenopus oocytes. Nature *328*, 80–82.

Mitsui, K., Tokuzawa, Y., Itoh, H., Segawa, K., Murakami, M., Takahashi, K., Maruyama, M., Maeda, M., and Yamanaka, S. (2003). The homeoprotein Nanog is required for maintenance of pluripotency in mouse epiblast and ES cells. Cell *113*, 631–642.

Morris, S.A. (2011). Cell fate in the early mouse embryo: sorting out the influence of developmental history on lineage choice. Reprod. Biomed. Online *22*, 521–524.

Morris, S.A., Teo, R.T., Li, H., Robson, P., Glover, D.M., and Zernicka-Goetz, M. (2010). Origin and formation of the first two distinct cell types of the inner cell mass in the mouse embryo. Proc. Natl. Acad. Sci. USA *107*, 6364–6369.

Neuman-Silberberg, F.S., and Schüpbach, T. (1993). The Drosophila dorsoventral patterning gene gurken produces a dorsally localized RNA and encodes a TGF alpha-like protein. Cell *75*, 165–174.

Nishioka, N., Yamamoto, S., Kiyonari, H., Sato, H., Sawada, A., Ota, M., Nakao, K., and Sasaki, H. (2008). Tead4 is required for specification of trophectoderm in pre-implantation mouse embryos. Mech. Dev. *125*, 270–283.

Nishioka, N., Inoue, K., Adachi, K., Kiyonari, H., Ota, M., Ralston, A., Yabuta, N., Hirahara, S., Stephenson, R.O., Ogonuki, N., et al. (2009). The Hippo signaling pathway components Lats and Yap pattern Tead4 activity to distinguish mouse trophectoderm from inner cell mass. Dev. Cell *16*, 398–410.

Niwa, H., Toyooka, Y., Shimosato, D., Strumpf, D., Takahashi, K., Yagi, R., and Rossant, J. (2005). Interaction between Oct3/4 and Cdx2 determines trophectoderm differentiation. Cell *123*, 917–929.

Palmieri, S.L., Peter, W., Hess, H., and Schöler, H.R. (1994). Oct-4 transcription factor is differentially expressed in the mouse embryo during establishment of the first two extraembryonic cell lineages involved in implantation. Dev. Biol. *166*, 259–267.

Park, H.Y., Trcek, T., Wells, A.L., Chao, J.A., and Singer, R.H. (2012). An unbiased analysis method to quantify mRNA localization reveals its correlation with cell motility. Cell Rep. *1*, 179–184.

Plusa, B., Frankenberg, S., Chalmers, A., Hadjantonakis, A.K., Moore, C.A., Papalopulu, N., Papaioannou, V.E., Glover, D.M., and Zernicka-Goetz, M. (2005). Downregulation of Par3 and aPKC function directs cells towards the ICM in the preimplantation mouse embryo. J. Cell Sci. *118*, 505–515.

Ralston, A., and Rossant, J. (2008). Cdx2 acts downstream of cell polarization to cell-autonomously promote trophectoderm fate in the early mouse embryo. Dev. Biol. *313*, 614–629.

Russ, A.P., Wattler, S., Colledge, W.H., Aparicio, S.A., Carlton, M.B., Pearce, J.J., Barton, S.C., Surani, M.A., Ryan, K., Nehls, M.C., et al. (2000). Eomesodermin is required for mouse trophoblast development and mesoderm formation. Nature *404*, 95–99.

Simmonds, A.J., dosSantos, G., Livne-Bar, I., and Krause, H.M. (2001). Apical localization of wingless transcripts is required for wingless signaling. Cell *105*, 197–207.

St Johnston, D. (2005). Moving messages: the intracellular localization of mRNAs. Nat. Rev. Mol. Cell Biol. *6*, 363–375.

Strumpf, D., Mao, C.A., Yamanaka, Y., Ralston, A., Chawengsaksophak, K., Beck, F., and Rossant, J. (2005). Cdx2 is required for correct cell fate specification and differentiation of trophectoderm in the mouse blastocyst. Development *132*, 2093–2102.

Sutherland, A.E., Speed, T.P., and Calarco, P.G. (1990). Inner cell allocation in the mouse morula: the role of oriented division during fourth cleavage. Dev. Biol. *137*, 13–25.

Yagi, R., Kohn, M.J., Karavanova, I., Kaneko, K.J., Vullhorst, D., DePamphilis, M.L., and Buonanno, A. (2007). Transcription factor TEAD4 specifies the trophectoderm lineage at the beginning of mammalian development. Development *134*, 3827–3836.

Yamanaka, Y. (2011). Response: Cell fate in the early mouse embryo—sorting out the influence of developmental history on lineage choice. Reprod. Biomed. Online *22*, 525–527, discussion 528.

Wu, G., Gentile, L., Fuchikami, T., Sutter, J., Psathaki, K., Esteves, T.C., Araúzo-Bravo, M.J., Ortmeier, C., Verberk, G., Abe, K., and Schöler, H.R. (2010). Initiation of trophectoderm lineage specification in mouse embryos is independent of Cdx2. Development *137*, 4159–4169.

Zernicka-Goetz, M., Pines, J., McLean Hunter, S., Dixon, J.P.C., Siemering, K.R., Haseloff, J., and Evans, M.J. (1997). Following cell fate in the living mouse embryo. Development *124*, 1133–1137.

Cell PRESS
Open ACCESS

EXTENDED EXPERIMENTAL PROCEDURES

Image Analysis

For quantification of spatial distribution of *Cdx2* transcripts represented as the polarization index (PI) of FISH signal, the algorithm described before (Park et al., 2012) was adopted and implemented in JRuby as an ImageJ plugin or in Matlab using MathWorks. Polar coordinates for individual cells were expressed as a single point defined by vector PI and angle θ on a polar graph (lower part of panel). PI vector is defined by the center of gravity of the cell and the center of gravity of the FISH signal. This vector shows an angular displacement, θ (the angular coordinate), from the apical-basal (polar) axis. The radial co-ordinate (PI) can be alternatively expressed along the apical-basal (polar) axis as the value BA. Positive and negative BA values mean that the polarization vector is directed toward the apical or basal side of the embryo, respectively (Figure 1).

Fluorescence intensity plots were derived using Matlab. Fluorescent signal was summed within a cell normal to the basal-apical axis and each profile was normalized to give a total intensity of 1, before being smoothed using a moving average filter of ten pixels (Figure S1). Threshold values were determined and applied by taking the mean pixel intensity of the profile plus one standard deviation, to remove spurious data points.

Deconvolution of the acquired time-lapse images was performed with 'Huygens Professional' (Scientific Volume Imaging), adopting a signal/noise per channel ratio of 10 with automatic search for background option, to yield micrographs used in figures.

Drug Treatments

The microtubule cytoskeleton was depolymerized by addition of Nocodazole (Sigma) to KSOM culture media (final concentration of 30 μM) and embryos cultured in drops under paraffin oil, for 30 min. The actin network was disrupted by addition of Cytochalasin D (Sigma) at a final concentration of 0.5 μg/μl and embryos cultured for 60 min. To study the effect of aPKC inhibition, 8-cell embryos were incubated for 1h in M2 medium containing 60nM GÖ6983 (Sigma). To induce compaction of the 4-cell embryos, these were incubated for 30-60 min in the presence of 200 μM diacylglycerol analog, DiC8 (Sigma). Embryos were fixed immediately after the drug treatment (see below). Control embryos, for each drug treatment, were cultured in the appropriate concentration, for the drug treatment, of DMSO as a vehicle control.

qRT-PCR on Outside and Inside Cells

Embryos were collected into M2 medium containing 4mg/ml BSA 76h post hCG (8-cell stage) and observed to have undertaken eight- to 16-cell-stage divisions, before being incubated in M2 with a fluorescently labeled microsphere suspension diluted to 1:50 for 30 s. Embryos were subsequently disaggregated in divalent cations-free M2 medium with careful and gentle pipetting. Three to four outside (fluorescently labeled) and inside (unlabelled) cells from individual embryos were isolated under the fluorescent dissecting scope, released into a cell lysis buffer (PicoPure RNA isolation kit, Arcturus) and frozen on dry ice. RNA was isolated according to the manufacturer's protocol and qRT-PCR performed as described earlier (Jedrusik et al., 2008).

RNA FISH Probes

Probes for *Cdx2* were made using PCR-generated DNA template derived using *Cdx2*F1/*Cdx2*R1T7 primer pairs for anti-sense probe and *Cdx2*F1T7/*Cdx2*R1 primers for the sense probe (*Cdx2*F1—TCGCCACCATGTACGTGAGCTACCT; *Cdx2*R1—TTCAGACCAC GGGAGGGGTCACTG; *Cdx2*F1T7—TAATACGACTCACTATAGGGATGTACGTGAGCTACCTTC; *Cdx2*R1T7—TAATACGACTCAC TATAGGGAGGGGTCACTGGGTGACAG). A probe for Gata3 was generated using pBluescript plasmid containing EcoRI/EcoRI fragment of mouse Gata3 (generous gift of Dr. Katrin Ottersbach, Cambridge, UK) linearized with XbaI as a template. A probe for Dab2 was prepared using the pOTB7 plasmid containing full-length human Dab2 cDNA (kindly provided by Dr Folma Buss, Cambridge, UK) linearized with EcoRI. A probe for Sox2 was generated using a 430 bp cDNA fragment cloned into pBSK plasmid as a template.

Antibodies for Immunofluorescence

Primary antibodies used for immunofluorescence: mouse anti α-tubulin monoclonal antibody (SIGMA, T9026, 1:500), rabbit anti-aPKC-ζ polyclonal IgG (Santa-Cruz Biotechnology, Inc. sc-216, 1:200), mouse anti-*Cdx2* (Biogenex, 1:200), goat anti-Sox17 (R&D Systems, 1:400), rabbit anti-Nanog (ReproCELL, 1:400), rabbit anti-FLOPED (1 μg/ml; generous gift from Jurrien Dean laboratory). Secondary antibodies: Alexa Fluor® 488 donkey anti-rabbit IgG (Invitrogen, A21206, 1:500), Alexa Fluor® 568 donkey anti-rabbit (Invitrogen, A10042, 1:500), Alexa Fluor® 647 donkey anti-rabbit IgG (Invitrogen, A31573, 1:500), Alexa Fluor® 488 goat anti-mouse IgG (Invitrogen, A 11029 1:500), Alexa Fluor® 647 donkey anti-mouse IgG (Invitrogen, A31571, 1:500), Alexa Fluor® 568 goat anti-rat IgG (Invitrogen, A11077, 1:500). Actin was visualized by incubation of embryos with Texas Red-X phalloidin (Invitogen, T7471) and Alexa Fluor® 647 phalloidin (Invitrogen, A22287) at a dilution of 1:50 in PBS for 30min.

Sequence Analysis

The secondary structure of mRNA was predicted and visualized using the RNAfold program (http://rna.tbi.univie.ac.at/) using default parameters (Mathews et al., 1999; Zuker, 2003). Sequences of *Cdx2* gene from various species were obtained from the UCSC Genome Bioinformatics Site (http://genome.ucsc.edu/) and aligned using ClustalW2 (http://www.ebi.ac.uk/Tools/clustalw2/). Evolutionary conservation was visualized using BoxShade 3.21 (http://www.ch.embnet.org/software/BOX_form.html).

Cell PRESS
Open ACCESS

SUPPLEMENTAL REFERENCES

Mathews, D.H., Sabina, J., Zuker, M., and Turner, D.H. (1999). Expanded sequence dependence of thermodynamic parameters improves prediction of RNA secondary structure. J. Mol. Biol. *288*, 911–940.

Zuker, M. (2003). Mfold web server for nucleic acid folding and hybridization prediction. Nucleic Acids Res. *31*, 3406–3415.

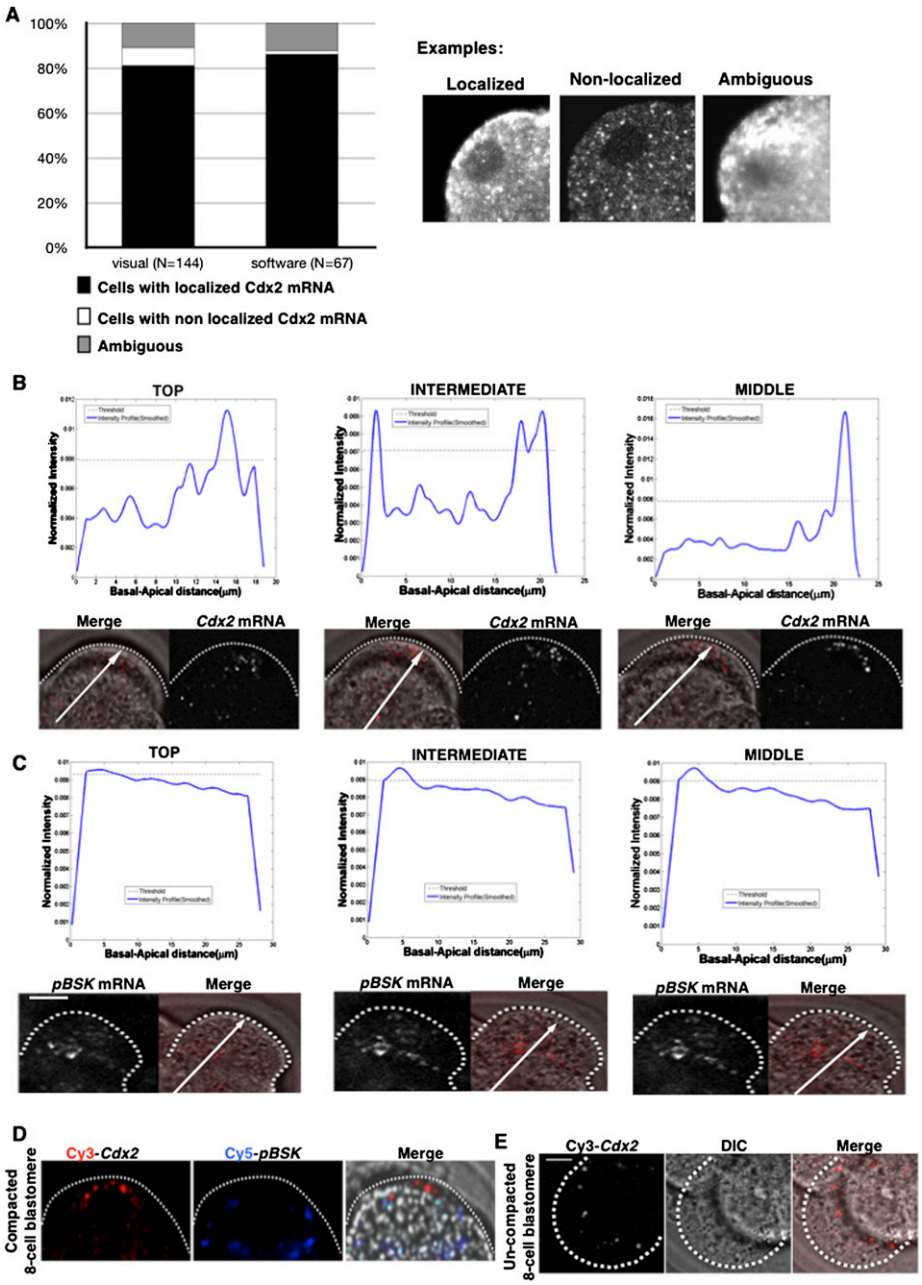

Figure S1. Localization of Endogenous and Exogenous *Cdx2* mRNA in Eight-Cell-Stage Embryos, Related to Figure 1

(A) Quantification of blastomeres showing apical localization of endogenous *Cdx2* mRNA by FISH in eight-cell-stage embryos, using visual observation and using the image analysis software. In the latter method, blastomeres were categorized based on the angle (θ) between the basal-apical axis of the blastomere and the polarization vector of the FISH staining as: showing apical localization for $\theta \leq 45$ deg, ambiguous for $45 < \theta < 90$ deg, and not showing apical localization for $\theta >= 90$ deg. Note, the two methods being equally good in detecting apically localized *Cdx2* transcripts. Examples of the three categories are shown on the right.

(B and C) Fluorescence intensity plots along the apical-basal axis derived for top, intermediate, and middle focal planes from confocal images of full-length *Cdx2* mRNA (B) and control RNA (C), injected into compacted eight-cell-stage blastomeres. Notice the prevalent peak at the position corresponding the apical side of blastomere. For the most cortical plane the cell curvature leads to the appearance of two peaks one at the projected basal side and one at the apical side.

(D) Coinjection of full-length wt *Cdx2* mRNA and RNA transcribed from the pBluescript vector, labeled with two different fluorescent dyes into compacted eight-cell blastomeres results in partitioning of the two RNAs similarly to single injections (see Figure 1). Scale bar, 5 μm.

(E) Injection of full-length wt *Cdx2* mRNA to precompacted eight-cell blastomere does not result in the apical localization of the transcripts.

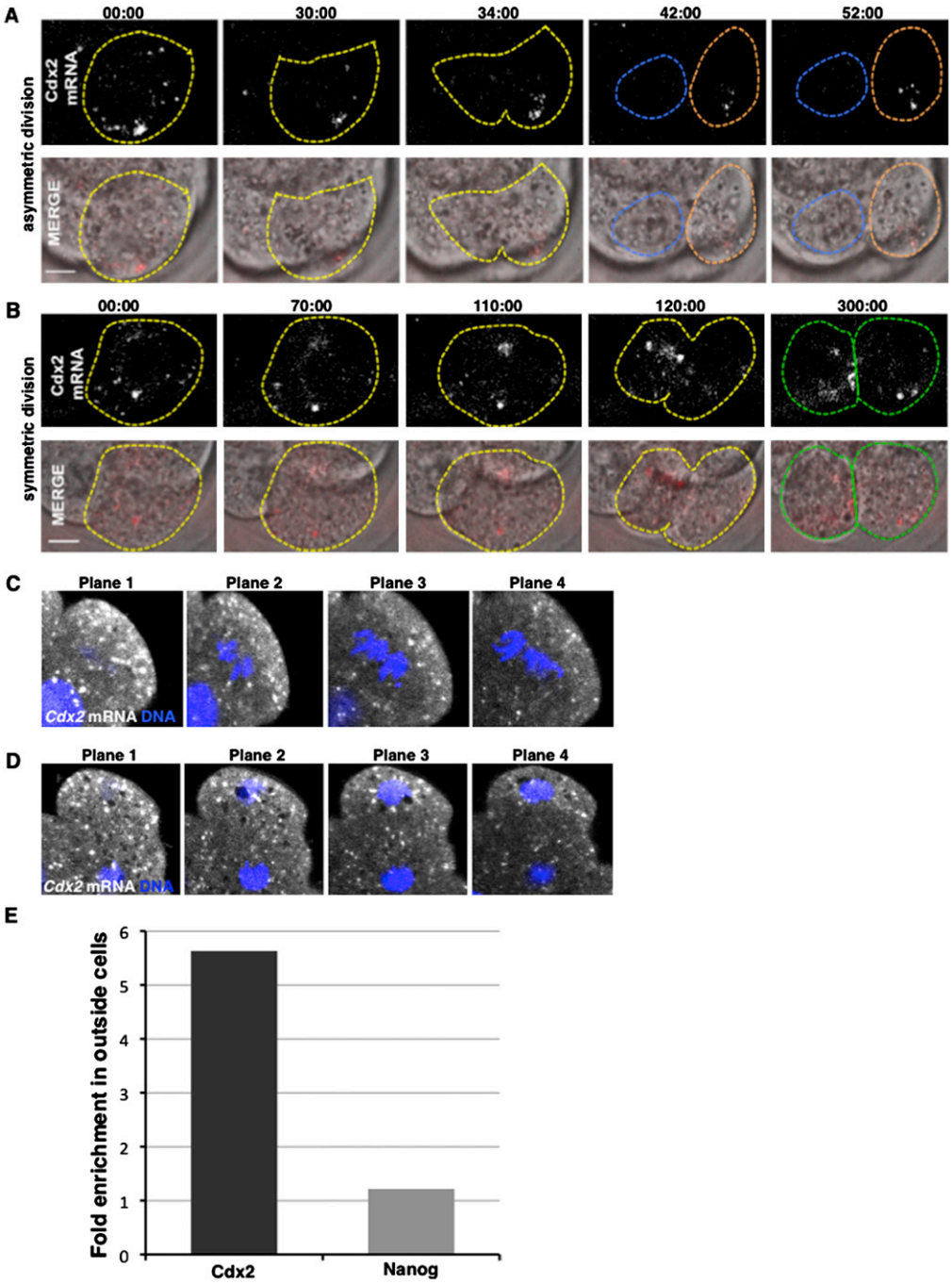

Figure S2. Inheritance of *Cdx2* mRNA during Eight- to 16-Cell Division, Related to Figure 2

(A and B) Time-lapse imaging of asymmetric (A) and symmetric divisions (B). Time-points (in hh:mm:ss format) were as indicated above the panels. Upper row shows the images taken in the red channel that results from the fluorescence of the Cy3-labeled *Cdx2* mRNA. Lower panels represent the merge of the DIC and red channels. Note that outside cells inherits majority of the labeled mRNA during differentiative cell division, while both cells arising from conservative division inherit comparable amounts of the RNA. Cell boundaries highlighted in dashed lines. Scale bar, 10 μm.

(C and D) Localization of *Cdx2* mRNA detected by FISH (white) in the eight-to-16 transiting cell. Four different focal planes are shown. DNA (blue) is stained with DAPI.

(E) Relative amounts of *Cdx2* and *Nanog* mRNAs measured by qRT-PCR in outside and inside cells isolated after the eight-to-16 cell division. Bars represent the average fold enrichment of particular mRNA in outside cells (14 samples of three to four cells) as compared with inside cells (nine samples of three to four cells).

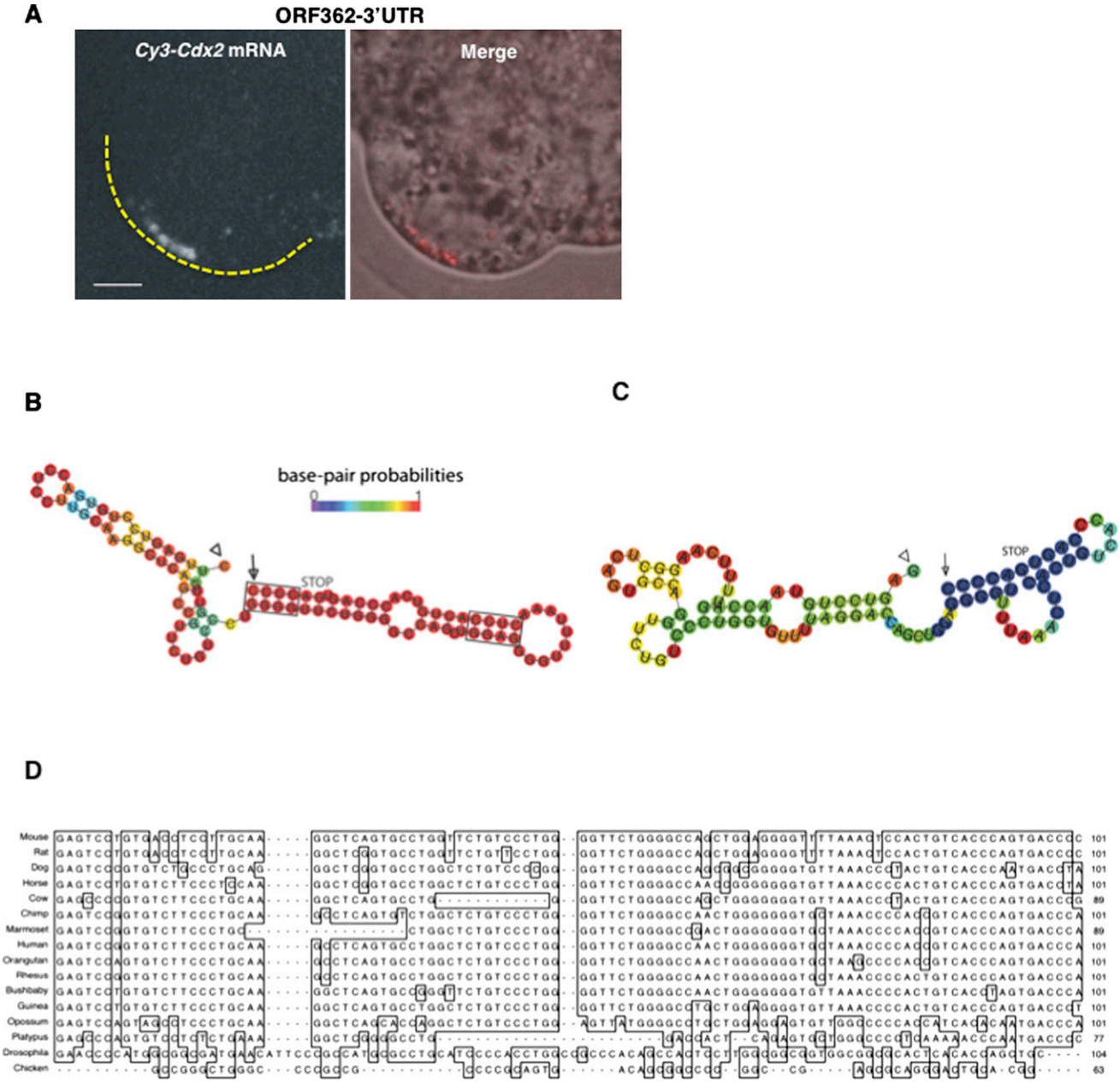

Figure S3. Localization Element of *Cdx2* mRNA, Related to Figure 3

(A) Fluorescently labeled RNA comprising 362 bases from 3′ of *Cdx2* ORF and the whole 3′UTR localizes apically upon injection to compacted eight-cell blastomere (n = 12/18).

(B and C) RNA secondary structure prediction of the (B) WT and (C) mutated form of the 97 bases element from the 3′ end of the *Cdx2* coding sequence (plus 4 additional bases after stop codon); arrow head and arrow mark the 5′ and 3′ end of RNA, respectively; base-pair probabilities are color coded. Runs of purins in WT version are boxed.

(D) The 97 bases long 3′ terminal part of *Cdx2* coding sequence (including codon stop) is highly conserved in live-bearing, especially placental, mammals but not in monotremes or lower vertebrates and invertebrates.

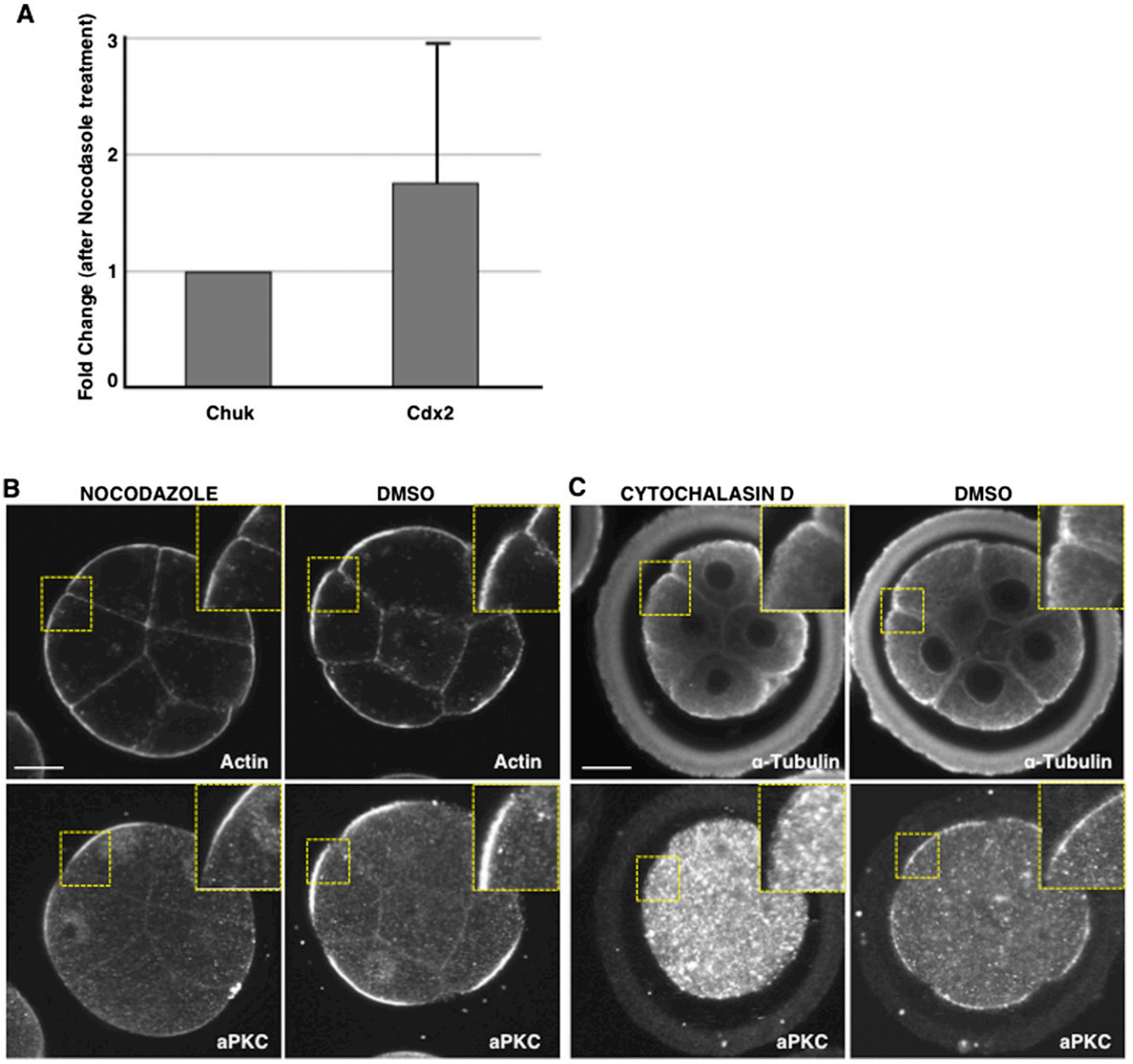

Figure S4. Effect of Cytoskeleton Disruption on *Cdx2* mRNA Expression and aPKC Localization, Related to Figure 4

(A) Quantitative RT- PCR was performed to embryos treated with 30 mM Nocodazole for 30 min and to the DMSO vehicle control group. Normalization was done against the gene *Chuk*. The Fold change between the Nocodazole treated group and the untreated group is shown. There is no significant difference in *Cdx2* transcripts level between the treated and the untreated group (Pair Wise Fixed Reallocation Randomization Test, P(H1) = 0.12). Data represent the average of two biological replicates.

(B and C) Embryos treated with Nocodazole (B) and Cytochalasin D (C) and with the vehicle control (DMSO). F-actin staining with phalloidin (upper panels in (B) and immunostaining for α-tubulin (upper panels in (C). Immunostaining for aPKC (lower panels in (B) and (C); Note - the differences in aPKC staining of control embryos in (B) and (C) result from different fixation protocols used in the two experiments. In panel (C), methanol fixation was used to preserve microtubules and this resulted in non-specific staining of the zona. Scale bar, 15 μm.

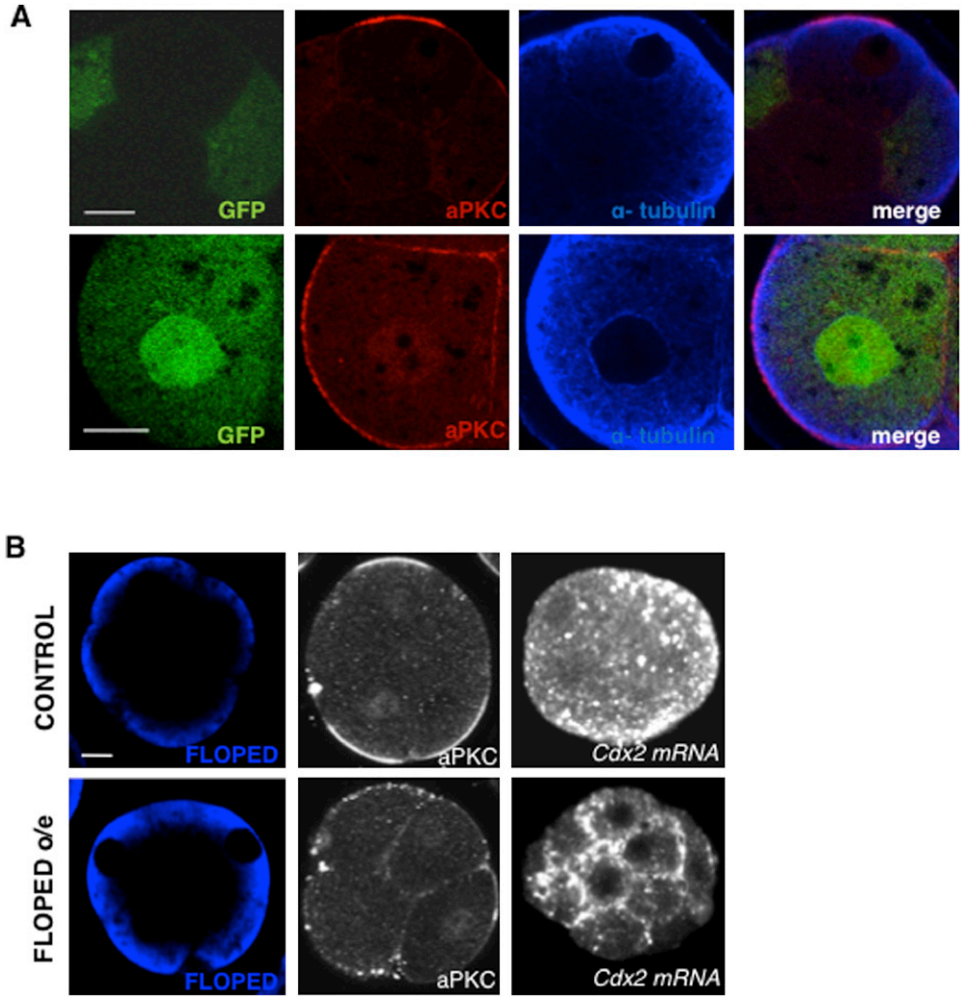

Figure S5. Overexpression of *dn-aPkc* and *Floped*, Related to Figure 5

(A) Effect of overexpression of dominant-negative (dn) form of aPKC on microtubule cytoskeleton. Both, injected and un-injected eight-cell stage blastomeres are shown (upper panels). Blow up of the dn-aPKC expressing blastomeres. Notice, disruption of the aPKC staining but not difference in alpha-tubulin staining (lower panels).

(B) Effect of overexpression of Floped protein on localization of aPKC and *Cdx2* mRNA in compacted eight-cell stage embryos.

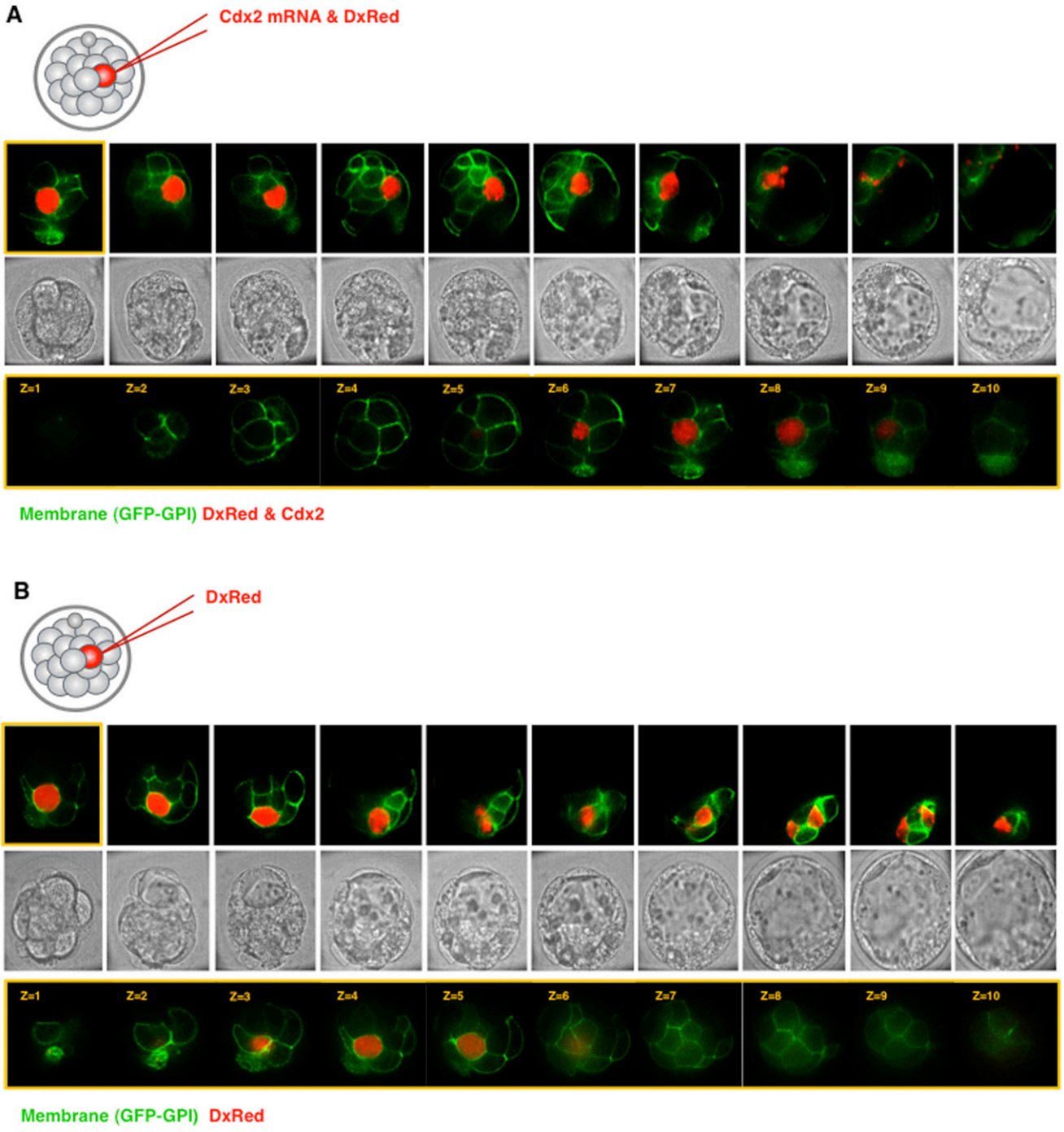

Figure S6. Overexpression of *Cdx2* in the Inside Cells of a Morula-Stage Embryo, Related to Figure 6

(A and B) Time-lapse series of a typical embryo with one inside cell injected with either *Cdx2* mRNA and dextran red – DxRed – (A) or DxRed alone (B). Embryos are expressing membrane form of GFP (green) to visualize cell boundaries to track cell behavior.